PROCEEDINGS OF A WORKSHOP ON COUNTY HYDROLOGY MANUALS

Edited by Dr. Johannes J. DeVries

Sponsored by

Water Resources Center
University of California

August 16-17, 1990
Davis, California

Lighthouse Publications
Mission Viejo, CA 92692

DEVELOPMENT OF HYDROLOGY MANUALS FOR SOUTHERN CALIFORNIA COUNTIES: I. MODEL SELECTION II. MODEL CALIBRATION

T.V. Hromadka II, California State University, Fullerton, CA
R.H. McCuen, University of Maryland, College Park, MD

Abstract

For southern California watersheds, as is the case of most watersheds in the United States, rainfall-runoff data are relatively sparse such that the calibration of a hydrologic model is uncertain. With the large number and types of hydrologic models currently available, the choice of the "best" hydrologic model to use is not clear. Because of the limited data, the hydrologic model must be simple in order to validate parameter values and submodel algorithms. Due to the uncertainty in stream gage data frequency analysis, a level of confidence (e.g. 85%) should be chosen to provide a level of protection against a specified flood return frequency (e.g. 100-year). Due to the calibrated model range and distribution of possible outcomes caused by the uncertainty in modeling parameter values, the use of a regionally calibrated model at an ungaged catchment needs to address the probability that the hydrologic model estimate of flood quantities (e.g. peak flow rates) achieves the level of protection for a specified flood level. In the two papers, a design storm unit hydrograph model is selected (paper I); developed and calibrated with respect to model parameter values and with respect to runoff frequency tendencies (paper II) in order to address each of these issues.

---

1 Associate Professor, Department of Mathematics, California State University, Fullerton, California 92634 and Director of Water Resources Engineering, Williamson and Schmid, 17782 Sky Park Boulevard, Irvine, California 92714

2 Professor, Department of Civil Engineering, University of Maryland, College Park, Maryland 20742

II. MODEL CALIBRATION

RUNOFF HYDROGRAPH MODEL PARAMETERS

The design storm unit hydrograph model ("model") is based upon several parameters; namely, two loss rate parameters (a phi index coupled with a fixed percentage), an S-graph, catchment lag, storm pattern (shape, location of peak rainfalls, duration), depth-area (or depth-area-duration) adjustment, and the return frequency of rainfall.

Loss Function

The loss function, f(t), used in the "model" is defined by

$$f(t) = \begin{cases} \bar{Y}I(t), & \text{for } \bar{Y}I(t) < Fm \\ Fm, & \text{otherwise} \end{cases} \qquad (1)$$

where $\bar{Y}$ is the low loss fraction and Fm is a maximum loss rate defined by

$$Fm = \sum ap_j \, Fp_j \qquad (2)$$

where ap_j is the actual pervious area fraction with a corresponding maximum loss rate of Fp_j; the infiltration rate for impervious area is set at zero; and I(t) is the design storm rainfall intensity at storm time t.

The use of a constant percentage loss rate $\bar{Y}$ in Eq. 1 is reported in Scully and Bender (1969), Williams et al. (1980), and Schilling and Fuchs (1986). The use of a phi index (ϕ - index) method in effective rainfall calculations is also well-known (e.g., Kibler, 1982).

The low loss rate fraction is estimated from the SCS loss rate equation (U.S. Dept. of Agric., 1972) by

$$\bar{Y} = 1-Y \qquad (3)$$

where Y is the catchment yield computed by

$$Y = \sum a_j Y_j \tag{4}$$

In Eq. 4, Y_j is the yield corresponding to the catchment area fraction a_j and is estimated using the SCS curve number (CN) by

$$Y_j = \frac{(P_{24} - Ia)^2}{(P_{24} - Ia + S) P_{24}} \tag{5}$$

where P_{24} = the 24-hour T-year precipitation depth; Ia is the initial abstraction of Ia = 0.2S; and S = (1000/CN)-10.

From the above relationships, the low loss fraction, $\bar{Y}$, acts as a fixed loss rate percentage, whereas Fm serves as an upper bound to the possible values of $f(t) = \bar{Y}I(t)$.

Values for Fm are based on the actual pervious area cover percentage (a_p) and a maximum loss rate for the pervious area, F_p. Values for F_p are developed from rainfall-runoff calibration studies of several significant storm events for several watersheds within the region under study. Further discussions regarding the estimation of parameter values are contained in a subsequent section.

A distinct advantage afforded by the loss function of Eq. 1 over loss functions such as Green-Ampt or Horton is that the effect of the location of the peak rainfall intensities in the design storm pattern on the model peak flow rate (Q) becomes negligible. That is, front-loaded, middle-loaded, and rear-loaded storm patterns all result in nearly equal peak flow estimates. Consequently, the shape (but not magnitude) of the design storm pattern is essentially eliminated from the list of parameters to be calibrated in the runoff hydrograph "model" (although the time distribution of runoff volumes are affected by the location of the peak rainfalls in the storm pattern which is a consideration in detention basin design).

S-Graph

The S-graph representation of the unit hydrograph (e.g., McCuen and Bondelid (1983), Chow and Kulandalswamy (1982), Mays and Coles (1980)) can be used to develop unit hydrographs corresponding to various watershed lag estimates. The S-graph was developed by rainfall-runoff calibration studies of several storms for several watersheds. By averaging the S-graphs for each watershed studied, a representative S-graph is developed for each watershed. By comparing the representative S-graphs, regional S-graphs were derived to represent the average of watershed-averaged S-graphs.

Lag

Fundamental to any hydrologic model is a catchment timing parameter. For the "model", watershed lag is defined as the time from the beginning of effective rainfall to that time corresponding to 50-percent of the S-graph ultimate discharge. To estimate catchment lag, it is assumed that lag is related to the catchment time of concentration (Tc) as calculated by a sum of normal depth flow calculated travel times; i.e., a mixed velocity method (e.g. Beard and Chang (1979), McCuen, et al. (1984)). To correlate lag to Tc estimates, lag values measured from watershed calibrated S-graphs were plotted against Tc estimates. A least-squares best fit line gives the estimator

$$\text{lag} = 0.80\text{Tc} \tag{6}$$

Design Storm Pattern

A 24-hour duration design storm composed of nested 5-minute unit intervals (with each principal duration nested within the next longer duration) was adopted as part of the policy. The storm pattern provides equal return frequency rainfalls for any storm duration; i.e., the peak 5-minute, 30-minute, 1-hour, 3-hour, 6-hour, 12-hour, and 24-hour duration rainfalls are all of the selected T-year return frequency. Such a storm pattern construction is found in HEC Training Document No. 15 (1982) which uses a nested central-loaded design storm pattern.

Runoff Hydrograph Model

The "model" produces a time distribution of runoff Q(t) given by the standard convolution integral representation of

$$Q(t) = \int_0^t e(s)\, u(t-s)\, ds \tag{7}$$

where Q(t) is the catchment flow rate at the point of concentration;

e(s) is the effective rainfall intensity; and u(x) is the unit hydrograph developed from the particular S-graph. In Eq. 7, e(s) represents the time distribution of the 24-hour duration design storm pattern modified according to depth-area effects and then further modified according to the loss function definition of Eq. 1.

In the use of Eq. 7 for a particular watershed, an estimate of catchment lag is used to construct a unit hydrograph u(x). Then, based on the catchment area (depth-area adjustment) and loss rate characteristics, e(s) is determined. Because the peak flow rate Q_p = max Q(t) shows a negligible variation due to a change in storm pattern shape (except for a severe front loaded, near-monotonically decreasing pattern or a rear loaded, near-monotonically increasing pattern); the model parameters that affect Q_p are loss rates ($\bar{Y}$ and F_p), S graphs, lag estimates, depth-area adjustment curve set, and design storm rainfall return frequency. Note that Fm is not a calibration parameter as Fm = $a_p F_p$ where a_p is the actual measured pervious area fraction.

PARAMETER CALIBRATION

Considerable rainfall-runoff calibration data has been prepared by the Corps of Engineers COE for use in their flood control design and planning studies. Much of this information has been prepared during the course of routine flood control studies in Orange County and Los Angeles County, but additional information has been compiled in preliminary form for ongoing COE studies for the massive Santa Ana River project (Los Angeles County Drainage Area, or LACDA). The watershed information available

includes rainfall-runoff calibration results for three or more significant storms for each watershed, developing optimized estimates for the S-graph, lag, and loss rate at the peak rainfall intensities. Although the COE used a more rational Horton type loss function which decreases with time, only the loss rate that occurred during the peak storm rainfalls was used in the calibration effort reported herein.

A total of 12 watersheds were considered in detail for our study. Seven of the watersheds are located in Los Angeles County while the other five catchments are in Orange County (Fig. 1). Several other local watersheds were also considered in light of previous COE studies that resulted in additional estimates of loss rates, S-graphs, and lag values. Table 1 provides an itemization of data obtained from the COE studies, and watershed data assumed for catchments considered hydrologically similar to the COE study catchments.

TABLE 1. WATERSHED CHARACTERISTICS

Watershed Name	Watershed Geometry: Area (mi^2)	Length (mi)	Length of Centroid (mi)	Slope (ft/mi)	Percent Impervious (%)	Tc (Hrs)	Calibration Results: Storm Date	Peak F_p (inch/hr)	Lag (hrs)	Basin factor
Alhambra Wash[1]	13.67	8.62	4.17	82.4	45	0.89	Feb.78 Mar.78 Feb.80	0.59,0.24 0.35,0.29 0.24	0.62	0.015
Compton2[1]	24.66	12.69	6.63	13.8	55	2.22	Feb.78 Mar.78 Feb.80	0.36 0.29 0.44	0.94	0.015
Verdugo Wash[1]	26.8	10.98	5.49	316.9	20	--	Feb.78	0.65	0.64	0.016
Limekiln[1]	10.3	7.77	3.41	295.7	25	--	Feb.78 Feb.80	0.27 0.27	0.73	0.026
San Jose[2]	83.4	23.00	8.5	60.0	18		Feb.78 Feb.80	0.20 0.39	1.66	0.020
Sepulveda[2]	152.0	19.0	9.0	143.0	24	--	Feb.78 Mar.78 Feb.80	0.22,0.21 0.32 0.42	1.12	0.017
Eaton Wash[1]	11.02[4] (57%)	8.14	3.41	90.9	40	1.05	---	---	---	0.015[7]
Rubio Wash[1]	12.20[5] (3%)	9.47	5.11	125.7	40	0.68	---	---	---	0.015[7]
Arcadia Wash[1]	7.70[6] (14%)	5.87	3.03	156.7	45	0.60	---	---	---	0.015[8]
Compton1[1]	15.08	9.47	3.79	14.3	55	1.92	---	---	---	0.015[8]
Dominguez[1]	37.30	11.36	4.92	7.9	60	2.08	---	---	---	0.015[8]
Santa Ana Delhi[3]	17.6	8.71	4.17	16.0	40	1.73	---	---	---	0.053[9] 0.040[10]
Westminster[3]	6.7	5.65	1.39	13	40		---	---	---	0.079[9] 0.040[10]
El Modena-Irvine[3]	11.9	6.34	2.69	52	40	0.78	---	---	---	0.028[9]
Garden Grove-Wintersberg[1]	20.8	11.74	4.73	10.6	64	1.98	---	---	---	---
San Diego Creek[1]	36.8	14.2	8.52	95.0	20	1.39	---	---	---	---

Notes 1: Watershed Geometry based on review of quadrangle maps and LACFCD strom drain maps.
2: Watershed Geometry based on COE LACOA Study.
3: Watershed Geometry based on COE Reconstitution Study for Santa Ana Delhi and Westminster Channels (June, 1983).
4: Area reduced 57% due to several debris basins and Eaton Wash Dam reservoir, and groundwater recharge ponds.
5: Area reduced 3% due to debris basin.
6: Area reduced 14% due to several debris basins.
7: 0.013 basin factor reported by COE (subarea characteristics, June, 1984).
8: 0.015 basin factor assumed due to similar watershed values of 0.015.
9: Average basin factor computed from reconstitution studies
10: COE recommended basin factor for flood flows.

Catchment Descriptions

The key catchments utilized for the calibration of the "model" design storm are Alhambra, Arcadia, Compton1 (at 120th Street), Compton2 (at Greenleaf), Dominguez, Eaton, and Rubio Washes. Although other watersheds were considered in the study (see Table 1) for the population of the parameter value distributions, the seven key catchments were considered similar to the region where the "model" is intended for use (the valley area of Orange County) and are used to develop flood frequency estimates.

Four of the seven catchments have been fully urbanized for 20 to 30 years, with efficient interior storm drain systems draining into a major concrete channel. Additionally, all of the major storm events have occurred during the gage record of full urbanization; hence, the gage record can be assumed to be essentially homogeneous (nevertheless, adjustments were made in this study to account for the urbanization effects). Storm drain system maps for the entire catchment were obtained from the Los Angeles County Flood Control District.

Arcadia and Rubio Washes were also fully urbanized and drained except for the foothill areas which account for 14% and 3% of the total catchment area, respectively. In both cases, debris dams (five in Arcadia, one in Rubio) intercept the foothill (most upstream area of the catchment) runoff. The sensitivity of the "model" results to including the foothill area without debris dams versus excluding the foothill area entirely are minor. Due to the increased loss rates and overall catchment lag, inclusion or exclusion of the foothill areas result in less than a ±5% variation in runoff estimates from the "model". Hence, the foothill area was excluded from each of the catchment analysis.

Eaton Wash is also fully urbanized and drained except for 57% of the total catchment area which is upstream of the Eaton Wash dam and water conservation spreading grounds. A review of the dam operation records indicated that the Eaton Wash stream gage record was impacted by outflows from the Eaton Wash dam by only three storms of the 27 year record (1969, 1980 and 1983 storms). The stream gage record was therefore modified according to the dam outflow hydrographs for these three storms. Hence, only the fully urbanized portion of Eaton Wash was used for the "model" calibration purposes.

Although all seven catchments are within a close vicinity of each other, they are located in two distinct groupings. Compton1, Compton2 and Dominguez are all neighboring catchments; whereas Arcadia, Alhambra, Eaton, and Rubio Washes are all located side-by-side with the same exposure to the incoming coastal storms. Because of the close similarities of the catchments in each of the two groupings, correlations between stream gage records are possible, which can then be used to supply any missing data points in the gage records or to check on the appropriateness of any adjustments made to the gage records due to dams, debris dams, or due to the effects of urbanization.

Peak Loss Rate, F_p

From Table 1, several peak rainfall loss rates are tabulated which include, when appropriate, two loss rates for double-peak storms. The range of values for all F_p estimates lie between 0.30 and 0.65 inch/hour with the highest value occurring in Verdugo Wash which has substantial open space in foothill areas. Except for Verdugo Wash, $0.20 \leq F_p \leq 0.60$ which is a variation in values of the order noted for Alhambra Wash alone. Figure 2 shows a histogram of F_p values for the several watersheds. It is evident from the figure that 88 percent of F_p values are between 0.20 and 0.45 inch/hour, with 77 percent of the values falling between 0.20 and 0.40 inch/hour. Consequently, a regional mean value of F_p equal to 0.30 inch/hour is proposed; this value contains nearly 80 percent of the F_p values, for all watersheds, for all storms, within 0.10 inch/hour.

S-Graph

Each of the watersheds listed in Table 1 has S-graphs developed for each of the storms where peak loss rate values were developed. For example, Fig. 3 shows the several S-graphs developed for Alhambra Wash. By averaging the several S-graph ordinates (developed from rainfall-runoff data), an average S-graph was obtained. By combining the several watershed average S-graphs (Fig. 4) into a single plot, an average of averaged S-graphs is obtained. This regionalized S-graph (Urban S-graph in Fig. 4) can be proposed as a regionalized S-graph for the several watersheds. Indeed, the variation in S-graphs for a single watershed for different storms (see Fig. 3) is of the order of magnitude

of variation seen between the several catchment averaged S-graphs. Such a regionalized S-graph can be developed for general regions classified as Valley, Foothill, Mountain, and Desert when the runoff data indicates similar tendencies. In this study, however, only the Valley region runoff data was considered.

In order to quantify the effects of variations in the S-graph due to variations in storms and in watersheds (i.e., for ungaged watersheds not included in the calibration data set), the scaling of Fig. 5 was used where the variable "X" signifies the average value of an arbitrary S-graph as a linear combination of the steepest and flattest S-graphs obtained. That is, all the S-graphs (all storms, all catchments) lie between the Feb. 1978 storm Alhambra S-graph (X = 1) and the San Jose S-graph (X = 0). To approximate a particular S-graph of the sample set,

$$S(X) = X\, S_1 + (1-X)\, S_2 \qquad (8)$$

where S(X) is the S graph as a function of X, and S_1 and S_2 are the Alhambra (Feb. 1978 storm) and San Jose S graphs, respectively. Figure 6 shows the population distribution of X where each watershed is weighted equally in the total distribution (i.e., each watershed is represented by an equal number of X entries). Table 2 lists the X values obtained from the Fig. 5 scalings of each catchment S-graph. In the table, an "upper" and "lower" X-value that corresponds to the X coordinate at 80 percent and 20 percent of ultimate discharge values, respectively, is listed. An average of the upper and lower X values is used in the population distribution of Fig. 6.

TABLE 2. CATCHMENT S-GRAPH X-VALUES

WATERSHED NAME	STORM	X(UPPER)	X(LOWER)	X(AVG)
Alhambra	Feb. 78	1.00	1.00	1.00
	Feb. 80	0.95	.60	0.78
	Mar. 78	0.70	.80	0.75
Limekiln	Feb. 78	0.50	0.80	0.65
	Feb. 80	0.80	1.00	0.90(2)
Supulveda	AVG.	0.90	0.80	0.85(3)
Compton	AVG.	0.90	1.00	0.95(3)
Westminster	AVG.	0.60	0.60	0.60(3)
Santa Ana Delhi	AVG.	0.80	1.00	0.90(3)
Urban	AVG.	0.90	0.80	0.85

In the table, the numbers in parenthesis indicate a weighting of the average X value. That is, due to only the average S-graph (previously derived by the COE) being available, it is weighted to be equally represented in the sample set with respect to the other catchments. All the catchments listed in the table are considered to be "Valley" type watersheds that are fully developed with only minor (if any) effects due to foothill terrain.

Catchment Lag

In Table 2, the Urban S-graph, which represents a regionalized S-graph for urbanized watersheds in valley type topography, has an associated X value of 0.85. When the Urban S-graph is compared to the standard SCS S-graph, a striking similarity is seen (Fig. 7). Because the new Urban S-graph is a near duplicate of the SCS S-graph, it was assumed that catchment lag (COE definition) is related to the catchment time of concentration, Tc, as is typically assumed in the SCS approach.

Catchment Tc values are estimated by subdividing the watershed into subareas with the initial subarea less than 10 acres and a flow-length of less than 1000 feet. Using a Kirpich formula, an initial subarea Tc is estimated, and a Q is calculated. By subsequent routing downstream of the peak flowrate (Q) through the various conveyances (using normal depth flow velocities) and adding estimated successive subarea contributions, a catchment Tc is estimated as the sum of travel times analogous to a mixed velocity method.

Lag values are developed directly from available COE calibration data, or by using "basin factor" calibrated from neighboring catchments (see Fig. 1). The COE standard lag formula is:

$$\text{lag (hours)} = 24\ n \left(\frac{L\ L_{ca}}{s^{0.5}} \right)^{0.38} \qquad (9)$$

where L is the watershed length in miles; L_{ca} is the length to the centroid along the watercourse in miles; s is the slope in ft/mile; and n is the basin factor.

Because Eaton Wash, Rubio Wash, Arcadia Wash and Alhambra Wash are all contiguous (see Fig. 1), have similar shape, slopes, development patterns, and drainage systems, the basin factor of n = 0.015 developed for Alhambra Wash was also used for the other three neighboring watersheds. Then the lag was estimated using Eq. 9.

Compton Creek has two gages, and the n = 0.015 developed for Compton2 was also used for the Compton1 gage. The Dominguez catchment, which is contiguous to Compton Creek, is also assumed to have a lag calculated from Eq. 9 using n = 0.015.

The Santa Ana-Delhi and Westminster catchment systems of Orange County have lag values developed from prior COE calibration studies. Figure 8 provides a summary of the local lag versus Tc data. A least-squares best fit results in

$$lag = 0.72Tc \tag{10}$$

McCuen et al. (1984) provide additional measured lag values and mixed velocity Tc estimates which, when lag is modified according to the COE definition, can be plotted with the local data such as shown in Fig. 9. A least-squares best fit results in:

$$lag = 0.80Tc \tag{11}$$

In comparison, McCuen (1982) gives standard SCS relationships between lag, Tc, and time-to-peak (Tp) which, when modified to the COE lag definition, results in:

$$lag = 0.77Tc \tag{12}$$

Adopting a lag of 0.80Tc as the estimator, the distribution of (lag/Tc) values with respect to Eq. 11 is shown in Fig. 10.

PARAMETER VERIFICATION

The three parameter distributions of loss rate F_p values, S-graph, and lag were used to simulate a severe storm of March 1, 1983, which was not included in the calibration set of storms. The March 1, 1983 storm was a multi-peaked storm event and the resulting model results for each of the Los Angeles watersheds are shown in Table 3.

The values for parameters used in the modeling results of Table 3 are F_p = 0.30 inch/hour; pervious cover = actual value; Urban S-graph; measured gage rainfall and storm pattern; and computed lag values from Eq. 11. Two sets of values for the low loss fraction, $\bar{Y}$, were used; namely (i) $\bar{Y}$ estimated from Eq. 3, and (ii) $\bar{Y}$ calibrated by taking $\bar{Y}$ equal to 1 - (measured storm runoff volume)/(measured storm rainfall). This second value of $\bar{Y}$ was calibrated (rather than using Eq. 3 due to the obvious variation in rainfall intensities over the watershed for the March 1 storm. Figure 11a provides a comparison between measured and modeled runoff hydrographs. Figure 11b shows the point rainfalls recorded at various gage locations. A comparison of Table 3 modeling results with other modeling results reported by Loague and Freeze (1985), HEC Research Note No. 6 (1979), and the HEC Technical Paper No. 59 (Abbott, 1978) shows that the subject modeling verification results are promising.

TABLE 3. MARCH 1, 1983, PEAK FLOW ESTIMATES

Watershed	Time (Hours)	Recorded Q(CFS)	Regional Model			Calibrated to Low Loss Fraction, $\bar{Y}$		
			Std. Time	Modeled Q(CFS)	Relative Error	Std. Time	Modeled Q(CFS)	Relative Error
Arcadia [1]	0615	1460	0655	1830	25	0655	1740	+19
	0845	3660	0900	3490	5	0900	3500	-4
	1215	4110	1215	1275	69	1250	1260	-69
	2000	1340	1925	3550	165	1925	3530	+163
Eaton [2,4]	0619	1780	0720	2005(+150)	13	0715	2320(+150)	+30
	0904	4300	0925	5420(+150)	26	0925	5510(+150)	+28
	1219	5430	1300	2570(+600)	53	1300	2830(+600)	-48
	1934	3080	1950	5160(+750)	68	1950	5310(+750)	+72
Rubio [3]	0630	1500	0700	2610	74	0700	2450	+63
	0900	3760	0905	5980	59	0905	5990	+59
	1215	2520	1245	2200	-13	1245	2110	-16
	1930	3520	1930	5920	68	1930	5900	+68
Alhambra	0615	2290	0710	2405	5	0710	2450	+7
	0830	7010	0915	6460	8	0915	6460	-8
	1200	5300	1255	1700	68	1255	2550	-52
	1900	5250	1940	5300	1	1940	5320	+1
Compton2	0645	3380	0645	1290	62	0645	1237	-63
	0815	4620	0940	4160	-10	0940	4100	-11
	1200	2430	1200	2460	1	1200	2320	-5
	1845	847	1955	970	14	2010	920	+9
Dominguez	0910	9830	0925	6915	30	0925	7600	-23
	1206	6180	1240	4180	32	1240	5000	-19
	1900	2400	1955	1735	28	1955	2090	-13
	2400	1700	2440	1905	12	2440	2370	+39

Notes: 1 - Area reduced 14% due to Debris Basins

2 - Area reduced 57% due to Eaton Dam

3 - Area reduced 3% due to Debris Basins

4 - ( ) added to modeled Q's to account for Eaton Wash Dam outflow (per LACFCD 1983 Storm Report)

PARAMETER UNCERTAINTY AND MODEL RESPONSE

The design storm/unit hydrograph model is to be used in Orange County for flood control study purposes. Due to the rapid urbanization of Orange County reflected in the local gage records, considerable uncertainty would result in modifying Orange County gage records for the effects of urbanization. In contrast, the Los Angeles gage records reflect nearly stable, fully developed conditions for over 30 years of record. Another important factor in the use of gage data is that the Orange County catchments typically have significant constrictions which severely impact the calibration of S-graphs and lag values but would be removed ultimately with further development.

In comparison, the Los Angeles gage records have nearly homogeneous gage records with free flowing, fully developed drainage systems. Additionally, the Los Angeles gages are within 10 miles of Orange County and are all subject to similar coastal influence. Consequently, the Orange County hydrology model is calibrated to the Los Angeles gage data, so that it can be transferred for use in Orange County watersheds. As a result, all parameter estimates from a standardized hydrology manual contain uncertainty. However, it is important to recognize that parameter estimates at a gage site are also uncertain, but the level of uncertainty would be much less than what occurs at an ungaged site.

Each of the "model" parameters (lag, F_p, and S-graph) for the Orange County watersheds are assumed to have the probability distribution functions (pdf) shown in a discrete histogram form in Figs. 2, 6, and 10 for F_p, S(X), and lag = 0.8Tc, respectively. For example, if the "model" is applied at a gaged site, say Alhambra Wash, then the

variability in the S graph is not given by Fig. 6 for S(X), where $0.60 \leq X \leq 1$, but for $0.75 \leq X \leq 1$ (see Table 2). Similarly, the estimate for lag is much more certain for Alhambra Wash than shown in Fig. 10. Consequently, the uncertainty in the "model" output for a gaged site will show a significantly smaller range in possible outcomes than if the total range of parameter values of Figs. 6 and 10 are assumed (as is done for the ungaged sites, or sites where an inadequate length of data exist for a constant level of watershed development).

In Orange County, it is assumed that any of the parameter values can take the values shown in Figs. 2, 6, and 10 with the indicated frequencies. That is, a particular watershed may respond equally likely as Alhambra Wash or Compton1, or any of the catchments used in the calibration effort. Because the several catchment parameter values vary and overlap, the overall frequency of parameter value occurrences are assumed given by the distributions shown.

To evaluate the "model" uncertainty, a simlulation that exhausts all combinations of parameter values shown in the pdf distribution was prepared. Because the lag/Tc plot is a function of Tc, several Tc values were assumed and lag values varied freely according to Fig. 10. The re-resulting Q/Qm distribution is shown in Fig. 12 for the case of Tc equal to 1 hour and a watershed area of 1 square mile (hence, depth-area adjustments are not involved). In the figure, Q is a possible model peak flow rate outcome, and Qm is the peak flow rate obtained from the "model" assuming lag equal to 0.8 Tc, F_p equal to 0.30 inch/hour, and X equal to 0.85 (Urban S-graph). The Q/Qm plots were all very close to Fig. 12 as a function of Tc; therefore, Fig. 12 is taken to represent the overall Q/Qm distribution for watershed areas less than 1 mi^2.

The results of Fig. 12 show that a flood control hydrology manual which stipulates a procedure for estimating peak flow rates has an associated Q/Qm distribution that represents the variation in possible true values of Q (if the parameters were known exactly) from the design value Qm used for flood control design purposes. This modeling uncertainty must be coupled to flood frequency estimate uncertainty in order to achieve a specified level of confidence that Qm provides a given level of flood protection.

Not reflected in Fig. 12 is the additional uncertainty due to the choice of depth-area adjustments. One frequently used set (e.g., HEC TD#15, 1982) is the NOAA Atlas 2 data, which provide adjustments for 30-minute, 1-, 3-, 6-, and 24-hour durations. Another candidate set of curves are the COE-developed Sierra-Madre storm depth-area adjustments for use in southern California. The variation in adjustment factors is shown in Fig. 13. With only two data points for a pdf distribution, a statistical evaluation is impossible. However, it is assumed that the COE adjustment factors are more appropriate for the southern California region than the NOAA Atlas 2 curves, which are 'regionalized' for the entire United States. Consequently, depth-area effects are being considered "exactly known" in a probabilistic sense, which implies (incorrectly) that there is no significant uncertainty in the adjustment factors used.

The effects on model certainty due to the choice of either set of depth-area relationships is reflected in Figs. 14-16. The figures show the distribution of Q/Qm for watershed areas of 5, 50, and 100 mi^2, respectively, and for an intermediate design storm frequency of 25 years.

In Fig. 15 it is seen that the COE depth-area curves result in such a significant adjustment of point rainfall values in the design storm that the Q/Qm range of outcomes is considerably less than when using the NOAA Atlas 2 set. That is, the error distribution of the "model" Q/Qm has a smaller range of values when using the COE depth-area curves than when using the NOAA Atlas 2 curves.

An important question arises as to whether or not the distribution of outcomes from the calibrated model can be reduced (i.e., the model made more certain) by introducing additional parameters. It is not clear in the current literature whether such a claim has validity. However, some pointed remarks can be taken from Klemes and Bulu (1979) who evaluate the "limited confidence in confidence limits derived by operational stochastic hydrologic models." They note that advocates of modeling "sidestep the real problem of modeling--the problem of how well a model is likely to reflect the future events--and divert the user to a more tractable, though less useful, problem of how best to construct a model that will reproduce the past events." In this fashion, "by the time the prospective modeler has dug himself out of the heaps of technicalities, he either will have forgotten what the true purpose of modeling is or will have invested so much effort into the modeling game that he would prefer to avoid questions about its relevance." Of special interest is their conclusion that "Confidence bands derived by more sophisticated models are likely to be wider than those derived by simple models." That is, "the quality of the model increases with its simplicity."

In a reply by Nash and Sutcliffe (1971) to comments by Fleming (1971), the simple model structure used by Nash and Sutcliffe (1971) is defended as to modeling completeness in comparison to the Stanford Watershed Model variant, HSP. Nash and Sutcliffe write that "...We believe that a simple model structure is not only desirable in itself but is essential if the parameter values of the component parts are to be determined reliably through an optimization procedure.... One must remember that the data always constitute a limited sample and the optimized values are 'statistics' derived from this sample and therefore subject to sampling variance. The more complex the model structure the greater is the difficulty in obtaining optimum parameter values with low sampling variance. This difficulty becomes particularly acute...when two or more model components are similar in their operation..."

Should a comparison be made between a simple model, such as described herein, and an 'advanced model', the results would not be conclusive. As Nash and Sutcliffe write that "...The more complex model would almost certainly provide a better fit, as a linear regression analysis on a large number of variables will almost invariably provide a better fit than one of those independent variables whose significance has been established." Hence, the hydrologist must be careful to evaluate modeling results obtained from a verification test rather than obtained from a calibration data set. Nash and Sutcliffe also note the dominating importance of errors in rainfall and effective rainfall estimates in complex models such as HSP: "We wonder, however, how the parameters expressing spatial variation of rainfall or infiltration capacity, can be optimized at all, let alone with stability or significance, in the typical case where the short-term rainfall data are based on a single recording rain gauge, as in Dr. Fleming's first example."

FLOOD FREQUENCY ANALYSIS

Adjustment for the Effects of Urbanization

In order to calibrate the design storm of the "model", flood frequency curve development was required. Seven of the Los Angeles County stream gage records show only minor effects due to urbanization and, therefore, required only a small amount of adjustment in order to develop a homogeneous gage record. The near homogeneity of the record is due to two major factors: (1) the watersheds have been fully urbanized for the last several decades, and (2) most of the major storms occurred during the period of full urbanization. The hydrologic stream gage adjustment procedure used for this study is presented in a paper by McCuen and Hromadka (1986).

With the stream gage data now adjusted for the effects of urbanization, a flood frequency analysis can be prepared. However, it is noted that uncertainty in the data adjustment procedure must exist due to the use of an adjustment model with a range of possible outcome values similar in concept to the Q/Qm distribution of Fig. 12. Therefore, in the choice of gage data for flood frequency analysis, the final results need to be evaluated in terms of a pdf about the so-called homogeneous gage record. Should the data require negligible adjustments, then the level of uncertainty introduced into the data by adjustments using an uncertain model is assumed to also be negligible. Because the data in our study required only a minor adjustment, no further investigation as to the distribution of this source of uncertainty was conducted.

Development of Confidence Intervals

Given several annual series of homogeneous stream gage data for the fully urbanized watersheds considered, a statistical analysis is needed to develop the confidence intervals for the flood design values of the several T-year return frequency floods (e.g., 2-year, 5-year,•••, 100-year).

The estimation of the T-year flood is a basic problem in hydrology due to the uncertainty caused by the uncertain estimation of parameters of the flood distribution. This uncertainty can have a significant effect on the flood design value, and its quantification is an important aspect of evaluating the risk involved in a choosen level of flood protection.

The Water Resources Council Bulletin 17B (1981) provide (in the case of a flood distribution whose logarithm is normally distributed) confidence intervals for the T-year flood by the use of the non-central student's t-distribution. The more general case, following the guidelines of Bulletin 17B, is when the logarithm of the flood distribution has a Pearson III distribution with a non-zero skew parameter. This case of non-zero skew is more complicated than the case of lognormally distributed floods, which is the case of zero skew (Bobee, 1979, 1973; Condie, 1977; Hardison, 1976; Kite, 1975, 1977; Stedinger, 1983). In an important paper, Stedinger (1983) shows that the confidence intervals, for quantiles, which are given in the U.S. Water Resources Council guidelines are not satisfactory. He uses a formula due to Kite (1975) and derives an expression for confidence intervals for the quantiles that he shows is satisfactory in several simulations.

Following the above developments, confidence intervals for the flood design values can be determined by simulation. The simulation gives an approximate sampling distribution and so can be used to obtain confidence intervals of various levels and can be also used to quantify the magnitudes and probabilities of various possible errors due to sampling.

Statistical Model Development

Zero skew. Consider the case where x, the logarithm of the maximum annual discharge, has a normal distribution. For the T-year flood, define the exceedance probability p by

$$p = 1 - 1/T \tag{13}$$

and let y_p be the p-th quantile of x:

$$P(x \leq y_p) = p \tag{14}$$

It is y_p that we want to estimate. If the mean μ and standard deviation σ of x were known, then since $(x-\mu)/\sigma$ has a N(0,1) distribution, i.e. a normal distribution with mean 0 and standard deviation 1,

$$(y_p - \mu)/\sigma = z_p \tag{15}$$

where z_p is the p-th quantile for an N(0,1) distribution. Of course, μ and σ are not actually known; we only have estimates for them, $\hat{\mu}$ and $\hat{\sigma}$, based on m data points for m years of gage data.

It follows that

$$(y_p - \hat{\mu})/\hat{\sigma} = ([(\mu - \hat{\mu})/\sigma] + z_p)/(\hat{\sigma}/\sigma). \qquad (16)$$

The random variable in brackets in Eq. 16 is distributed as $Z/\sqrt{m}$, where Z has a N(0,1) distribution, and the denominator of Eq. 16 is distributed as $\sqrt{W}$, where W has a chi-squared distribution with m-1 degrees of freedom, divided by m-1, which is independent of Z. Thus Eq. 16 can be written as

$$(1/\sqrt{m})[(Z + z_p\sqrt{m})/\sqrt{W}]. \qquad (17)$$

The random variable in brackets in Eq. 17 has a non-central t-distribution, with non-centrality parameter $\delta = z_p\sqrt{m}$; the special case $\delta = 0$ is the student's t-distribution (e.g. Breiman, 1973).

Since the distribution of (16) can be written in terms of the known non-central t-distribution, confidence intervals for y_p can be developed. For flood control study purposes, the confidence interval used is a one-sided interval that gives an upper bound. The choice of the value T, for the T-year flood, and the number m of data points (years of gage record) determine the non-centrality parameter δ. The other quantity that must be specified is a probability p' for the one-sided confidence interval. If $t_{p'}$ is the p'-th quantile of this non-central t-distribution, then

$$P(y_p \leq \hat{\mu} + \hat{\sigma}\,(t_{p'}/\sqrt{m})) = p' \qquad (18)$$

giving the one-sided 100p' percent confidence interval for y_p.

Non-zero skew. Let the logarithm x of the yearly peak discharge have a Pearson type III distribution with density function

$$f(x) = (1/|a|\Gamma(b))[(x-c)/a]^{b-1} \exp-[(x-c)/a] \qquad (19)$$

where, in the case of positive "a", the density is given by Eq. 19 for $x>c$ and is zero for $x<c$, while in the case of negative "a" the density is given by Eq. 19 for $x<c$ and is zero for $x>c$. Computing the mean μ, standard deviation σ, and skew γ from Eq. 19 gives (see, for example Hall, 1984)

$$\begin{aligned} \mu &= c + ab \\ \sigma^2 &= a^2 b \\ \gamma^2 &= 4/b, \end{aligned} \qquad (20)$$

where "a" has the same sign as γ.

In following the guidelines of Bulletin 17B, the skew coefficient γ is estimated either from a map of regional skew or from a large pool of data from that region. Consequently, the error in estimating γ is of an entirely different kind than that which arises in estimating μ and σ by means of m data points for the specific area for which the T-year flood is being estimated. Typically, the station skew differs considerably from the regional skew (resulting in significantly different flood frequency statistics) and a weighted average is developed. However, there is substantial uncertainty as to what the "true" skew is. To proceed with the development, it is assumed that the skew γ is given "exactly". What is thereby analyzed is that part of the variability in the estimate of the T-year flood that arises from the uncertainty in the estimation of μ and σ; this ignores the variability that comes from the

uncertainty in the estimate of γ. (As an example of the effects of the choice of skew, estimates for Q_{100} in Orange County varied by more than 60 percent depending on whether a station or regional skew is used.)

The form of the density Eq. 19 shows that the random variable

$$Z = (x-c)/a \tag{21}$$

has the one parameter density

$$g(x) = (1/\Gamma(b))x^{b-1}e^{-x} \tag{22}$$

for $x>0$ and 0 for $x<0$; i.e., Z has a gamma distribution with shape parameter b and scale parameter 1.

Introducing the constant K_p defined by

$$y_p = \mu + \sigma K_p. \tag{23}$$

then from Eq. 20,

$$\begin{aligned}(y_p - \mu)/\sigma &= (1/\sqrt{b})[(y_p - c)/a]-\sqrt{b} \text{ if } a>0\\ (y_p - \mu)/\sigma &= (1/\sqrt{b})[(y_p - c)/a]+\sqrt{b} \text{ if } a<0\end{aligned} \tag{24}$$

If t_q is the 100q-th percentile for the gamma distribution Z, then the choice q=p gives the first equation below for $a>0$, while the second equation follows from the choice q=1-p:

$$\begin{aligned}P((y_p - \mu)/\sigma \leq (t_p-b)/\sqrt{b}) &= p \text{ if } a>0\\ P((y_p - \mu)/\sigma \leq (b-t_{1-p}))/\sqrt{b}) &= p \text{ if } a>0.\end{aligned} \tag{25}$$

That is,

$$\begin{aligned}K_p &= (t_p-b)/\sqrt{b} \text{ for } a>0,\\ K_p &= (b-t_{1-p})/\sqrt{b} \text{ for } a<0.\end{aligned} \tag{26}$$

As in the case of zero skew,

$$(y_p - \hat{\mu})/\hat{\sigma} = \{[(\mu - \hat{\mu})/\sigma] + K_p\}/[\hat{\sigma}/\sigma] \tag{27}$$

This Eq. 27 shows that the joint distribution of the two random variables in brackets must be found. A substantial simplification can be obtained by writing both of these random variables in term of the Z of Eq. 21.

Let $X_1, \cdots, X_m$ be independent, each with a Pearson III distribution and let $Z_j = (X_j - c)/a$. Then

$$\hat{\mu} = (1/m)\,\Sigma X_j = (a/m)\{\Sigma\,((X_j - c)/a)\} + c = a\hat{\mu}_Z + c \tag{28}$$

where $\hat{\mu}_Z$ is the estimator for the mean of Z. The customary estimator for $\hat{\sigma}^2$ is:

$$\frac{\hat{\sigma}^2}{\sigma^2} = (1/ma^2b)\,\Sigma\,(X_j - \hat{\mu})^2 = (1/mb)\,\Sigma(Z_j - \hat{\mu}_Z)^2 = \hat{\sigma}_Z^2/b \tag{29}$$

where $\hat{\sigma}_Z^2$ is the customary estimator for the variance σ_Z^2 of Z. Using $\sqrt{(\hat{\sigma}^2/\sigma^2)}$ as the estimator for $\hat{\sigma}/\sigma$, Eq. 29 shows that this estimator is

$$\hat{\sigma}/\sigma = \hat{\sigma}_Z/\sqrt{b} \tag{30}$$

Similarly,

$$\begin{aligned} (\mu - \hat{\mu})/\sigma &= (b - \hat{\mu}_Z)/\sqrt{b} \text{ for } a > 0, \\ (\mu - \hat{\mu})/\sigma &= (\hat{\mu}_Z - b)/\sqrt{b} \text{ for } a < 0. \end{aligned} \tag{31}$$

Combining Eqs. 26, 27, 29, and 31 we obtain the final equation set:

$$\begin{aligned} (y_p - \hat{\mu})/\hat{\sigma} &= (t_p - \hat{\mu}_Z)/\hat{\sigma}_Z \text{ for } a > 0, \\ (y_p - \hat{\mu})/\hat{\sigma} &= (\hat{\mu}_Z - t_{1-p})/\hat{\sigma}_Z \text{ for } a < 0. \end{aligned} \tag{32}$$

So confidence intervals for y_p can be obtained if, for Z having the distribution of Eq. 22, we know the distribution of

$$(\delta - \hat{\mu}_Z)/\hat{\sigma}_Z. \tag{33}$$

Confidence intervals are then determined by simulation. Details of the simulation procedure and the computer code can be obtained in Whitley and Hromadka (1986a,b).

POLICY STATEMENT OBJECTIVE

In order to calibrate the "model" design storm so that the peak flow rate estimates represent local stream gage flood frequency tendencies, an objective for flood protection must be specified. That is, not only is a 100-year flood (for example) selected as a targeted level of flood protection, but also a level of confidence in estimating (or exceeding) the 100-year flood must be specified. This specification for a hydrologic model becomes part of the local agency's policy statement for flood control.

In this application, the policy statement objective is that an 85 percent confidence in design flow estimates be achieved:

$$P(Q_m^T \geq Q_T) = 0.85 \tag{34}$$

where Q_m^T is the T-year design storm unit hydrograph model peak flow rate, and Q_T is the "true" T-year flood flow rate. From the simulation of the adjusted stream gage data, several confidence levels in stream gage data for the Q_{100} estimates are listed in Table 4. Estimates of the T-year flood at a 85 percent confidence level are provided in Table 5.

TABLE 4. SIMULATION RESULTS IN ESTIMATING Q_{100}

record number of years	Watershed Name	Confidence Level Q(cfs) 25%	50%	75%	85%	95%
54	ALHAMBRA	7659	8280	9025	9488	10391
28	ARCADIA	4429	5029	5820	6354	7496
27	COMPTON1	5563	6227	7092	7669	8891
56	COMPTON2	7769	8455	9282	9798	10807
16	DOMINGUEZ	18262	21199	25388	28428	35526
28	EATON	6307	7066	8053	8712	10100
54	RUBIO	4667	4979	5348	5575	6012

TABLE 5. T-YEAR FLOOD ESTIMATES

Watershed Name	At 85% Confidence Level T-Year Flood 2	5	10	25	50	100
ALHAMBRA	3100	4543	5611	7078	8250	9488
ARCADIA	1610	2568	3330	4431	5351	6354
COMPTON1	2296	3473	4365	5606	6606	7669
COMPTON2	2899	4364	5489	7079	8386	9798
DOMINGUEZ	7702	12313	15820	20639	24454	28428
EATON	2566	3875	4882	6302	7463	8712
RUBIO	2152	3026	3627	4401	4986	5575

In the development of the confidence limit values of Tables 4 and 5, the computed skew used for each station is the Bulletin 17B recommended weighted average of a regional skew and station skew. Here, the station skew used is developed from the adjusted annual series (adjusted for urbanization effects), and the regional skew used is based on regionalization of the adjusted station skews (7 gages).

DESIGN STORM CALIBRATION

"Model" Parameters

Because of the choice of loss rates in Eq. 1, the location of the peak rainfalls in the design storm and the shape of the storm pattern are essentially removed as calibration variables in the "model" (there is some effect by arranging the design storm pattern to be monotonically increasing or decreasing; however, such a pattern is considered unlikely based on the typical shape of storm patterns observed). Additionally, the "model" can be calibrated to local flood frequency tendencies using only the following parameters: F_p equal to 0.30 inch/hour; a_p equal to actual measured pervious area fraction Urban S-graph (X equal to 0.85); lag equal to 0.8Tc; $\bar{Y}$ based on Eq. 3 using the SCS curve number and 24-hour storm precipitation; the COE depth-area curves; and the return frequency of the rainfall (T-year) used in the design storm.

Tc estimates are derived for each catchment (urbanized portions) using the summation of travel times. It was noted that when using preliminary estimates, which were eventually shown to be reasonably close to the final estimates, for T-year flow rates to calculate travel times, the variation in Tc values was minor, on the order of 10 percent, between 2-year and 100-year storm approximations. Estimates for a_p were obtained from COE calibration data and are held constant for all storms. $\bar{Y}$ varied according to the selected 24-hour precipitation and soil cover curve number (held constant). Finally, the S-graph, F_p equal to 0.30 inch/hour, and COE depth-area curves are "constants". Therefore, only one parameter is varied for the"model" calibration: the design storm return frequency (T-year).

Design Storm Calibration Procedure

For each of the seven catchments, values for Fm ($Fm = a_p F_p$), $\bar{Y}$ as a function of curve number and P_{24}, and lag were developed (see Table 6). Because lag varied only slightly for T-year storm estimates of Tc, a constant lag is used for each catchment.

The objective function, χ, used to calibrate the design storm is

$$\chi_T(t) = \frac{\sum_{i=1}^{m} (\hat{Q}_i^t - Q_i^T)\, A_i / Q_i^T}{\sum_{i=1}^{m} A_i} \qquad (35)$$

where $\chi_T(t)$ is the objective function considered at the T-year flood; $\hat{Q}_i^t$ is the "model" peak flow estimate for catchment i using a t-year design storm; Q_i^T is the catchment i 85 percent confidence level T-year flood computed from the adjusted stream gage data and the simulation procedure (see Table 5); and A_i is the catchment i area. Consequently, the objective function provides an area weighted fit of "model" relative errors in achieving the desired flood control level of protection.

The design storm of the "model" is calibrated for the T-year flood protection level by finding the t that satisfies

$$\chi_T(t) = 0 \qquad (36)$$

Figure 17 shows the variation in $\chi_T(t)$ as a function of t, for T = 2-, 5-, 10-, 25-, 50-, and 100-year events.

TABLE 6. MODEL PARAMETER VALUES

Watershed	a_p[1]	F_p(in/hr)	F_m(in/hr)	CN[2]	Low Loss Fraction ($\bar{Y}$)						LAG(hrs)[3]
					2 yr	5 yr	10 yr	25 yr	50 yr	100 yr	
Arcadia	0.55	0.30	0.165	56	0.53	0.45	0.41	0.37	0.35	0.32	0.48
Eaton	0.60	0.30	0.180	56	0.57	0.50	0.46	0.41	0.39	0.37	0.84
Rubio	0.60	0.30	0.180	56	0.56	0.49	0.44	0.40	0.38	0.35	0.54
Alhambra	0.55	0.30	0.165	56	0.53	0.46	0.43	0.39	0.36	0.34	0.71
Compton1	0.45	0.30	0.135	56	0.47	0.44	0.40	0.37	0.35	0.33	1.54
Compton2	0.45	0.30	0.135	56	0.47	0.44	0.40	0.37	0.35	0.33	1.78
Dominguez	0.40	0.28	0.112	61	0.43	0.37	0.34	0.31	0.29	0.27	1.66

Notes:

1) Map measured value
2) AMC II
3) LAG = 0.8Tc

ADDRESSING MODEL UNCERTAINTY

The design storm calibration results provide an area-averaged best fit of the objective function $\chi_T(t)$ such that $\chi_T(t)$ equals 0 for every return period T = 2, 5, 10, 25, 50, and 100 years. Model parameters are based on representative values selected from the parameter probability density functions (pdf) of Figs. 2, 6, and 10.

However, assuming that the true parameter value distributions are described by the several pdf, the "model" peak flow rate distribution is given by Figs. 14-16. Each of these figures indicates that approximately 57 percent of the possible "model" outcomes (peak flow rate, Q) are less than the "model" peak flow rate (Qm), i.e.,

$$P(Q_m \geq Q) = 0.57 \tag{37}$$

where Eq. 37 is essentially independent of the design storm frequency (T) and catchment area size.

To include the "model" uncertainty in the calibration process, another policy statement is required to specify the confidence level for $P(Q_m \geq Q)$. For example, should the policy be selected that the "model" provides a 100 percent chance that at least an 85 percent confidence level in T-year flood protection is achieved (in an area-averaged sense), then the effective rainfall must be increased in the design storm calibration results obtained using the Q_m estimates. That is, Figs. 14-16 indicate that there is only a 43 percent chance that Q_m provides at least the 85 percent confidence level, in T-year flood protection. Should the policy be selected that there be a 100 percent chance that Q_m provides at least the 85 percent confidence level, then $Q_m(t)$ must be increased so that the entire Q/Qm distribution lies above the 85 percent confidence level. That is, the price of model uncertainty is paid by

incorporating modeling conservatism and increased flood protection costs.

Given the above considerations, the subject of modeling uncertainty is "well-posed" for flood control policy makers in that the selection of an arbitrary hydrologic model for flood control planning and design needs to include the evaluation of model uncertainty due to the use of incorrect parameter values. In the choice of a particular model, therefore, it would be preferable to use a model that achieves a high probability of providing a selected level of flood protection with enough conservatism to compensate for modeling uncertainty. Consequently, the use of complex models that include several parameters whose values have a significant level of uncertainty may result in higher overall flood control costs in order to compensate for the overall modeling uncertainty.

Evaluating Model Uncertainty

From the above discussion a generalized procedure for evaluating model uncertainty can be specified by the following steps:

(1) Identify all model parameters and submodels (e.g., loss rate parameters and functions, hydraulic routing parameters and functions, etc.).

(2) Identify the range and probable distribution of values for each parameter. Included in this step is the demonstration of the "physics" of each submodel and possible range of parameter values needed to reasonably correlate the submodel to known responses (e.g., channel routing).

(3) Develop pdf plots for each parameter. Select a single representative value as an average value from each pdf. Should several subareas be used in the catchment schematic, each subarea must be represented by each parameter pdf used in

the subarea. Similarly, each routing link is represented by the associated parameter pdf plots.

(4) For each catchment, calculate Q_m by using the representative values for each parameter selected from step 3.

(5) Develop the Q/Q_m distribution by randomly selecting each parameter value set from the associated pdf plots (independently).

(6) Select a probability that the model achieves the desired level of flood protection.

(7) Calibrate Q_m so that the probability of step 6 is achieved.

It is noted that the considered "model" involves only three parameters in the uncertainty evaluation. Had a catchment been subdivided into several (say n) subareas, then 3n pdf distributions would be involved in the uncertainty study (along with pdf distributions for channel routing or any other submodel used). The model uncertainty issue can be interpreted by the use of Fig. 17. From the figure, the specified hydrology policy statement (Q_m) is an estimate of the true peak flow rate (Q) which would be developed assuming the design storm return frequency event. Figure 17 shows that due to the incorrect choice of model parameters (Tc, Fm, S-graph or X), the Q_m estimate for a catchment can be considerately higher than the actual peak flow rate generated from the catchment using the specified design storm return frequency. As a rseult, the use of the Q_m estimate in the calibration of the design storm will result in a lower design storm return frequency than had the actual peak flow rate been used.

To compensate for modeling uncertainty, the design storm calibration, can be refined to adjust the design storm return frequency such that the Q/Qm distribution is shifted to the right in Fig. 17 until the desired percentage of the Q/Qm distribution area lies above the targeted stream gage confidence level T-year Q estimates.

To develop the additional design storm calibrations, adjustment factors were determined (from Fig. 14-16) which reduce the Q_m estimates to achieve the 50-percent, 85-percent, and 100-percent levels of model certainty. These reduced Q_m estimates were then used in additional design storm calibrations using Eq. 35. The results of the several calibration efforts are shown in Fig. 18. Table 7 summarizes the design storm return frequencies needed to achieve the considered levels of model certainty. In Table 7, only AMC II conditions are considered in the $\bar{Y}$ estimations due to the low variation in model Q estimates due to variations in AMC. Table 8 summarizes (from Fig. 18) what level of model certainty is achieved in predicting the 85 percent confidence level for the T-year flood when using the T-year design storm. From Fig. 18 it is seen that depending on how certain one wants to be in estimating the 85 percent confidence level (for example) for the T-year flood, a wide range in design storm frequency is obtained. For example, a 10,000 year storm (in this study) would be needed to quarantee (at an ungaged site) that the 85 percent confidence level for the 100-year flood is estimated. In contrast, a 100-year design storm results in a 53 percent level of certainty that the 85 percent confidence level for the 100-year flood is estimated.

TABLE 7. DESIGN STORM FREQUENCY[1] NEEDED TO ACHIEVE 85 PERCENT CONFIDENCE LEVEL T-YEAR FLOOD FOR VARIOUS LEVELS OF MODEL CERTAINTY[2]

T-YEAR FLOOD	LEVEL OF MODEL CERTAINTY			
	43%	50%	85%	100%
2	2	2	3	6
5	4	5	6	25
10	7	9	20	80
25	17	20	60	400
50	30	37	150	2000
100	65	80	425	10000

Notes:

1 Using AMC II to compute $\bar{Y}$.

2 See Figure 18.

TABLE 8. MODEL CERTAINTY ACHIEVED USING T-YEAR DESIGN STORM FOR T-YEAR FLOOD (@ 85 PERCENT CONFIDENCE)

T-YEAR FLOOD	T-YEAR DESIGN STORM[1]	MODEL CERTAINTY ACHIEVED[2] (%)
2	2	30
5	5	57
10	10	58
25	25	62
50	50	57
100	100	53

Notes:

1 AMC II used to estimate $\bar{Y}$ (modeled peak Q variance to changes in AMC is small)

2 Satisfies Eq. 36.

THE POLICY STATEMENT FOR FLOOD CONTROL: THE HYDROLOGY MANUAL

After the level of flood control has been developed and the "model" calibrated, a policy statement for flood control can be prepared in the form of a Hydrology Manual. Such a document presents the mechanics in the use of the calibrated "model" so that the uncertainty in modeling results is not increased by misapplication. Parameter values and definitions, including maps, are included in the manual in order that identical parameter estimates can be determined by various parties.

CONCLUSIONS

A hydrology model for flood control design and planning has been developed that addresses the issues of uncertainty in stream gage data and statistics, and the uncertainty in model estimates. Because the coupling of these two uncertainties has not been addressed in the literature nor considered in the usual policy making procedures in flood control, it is suggested that it is important for flood control policy statements to include the specification of stream gage confidence levels and confidence in modeling predictions.

REFERENCES

1. Akan, A.O., and Yen, B.C., Diffusion-Wave Flood Routing in Channel Networks, Journal of The Hydraulics Division, ASCE, Vol. 107, No. HY6, June, 1981.

2. Alonso, C., Stochastic Models of Suspended-Sediment Dispersion, Journal of Hydraulic Engineering, Proceedings of the American Society of Civil Engineers, Vol. 107, No. HY6, June, 1981.

3. Beard, L., Impact of Hydrologic Uncertainties On Flood Insurance, Journal of The Hydraulics Division, ASCE, Vol. 104, No. HY11, November, 1978.

4. Beard, L. and Chang, S., Urbanization Impact on Streamflow, Journal of The Hydraulics Division, ASCE, Vol. 105, No. HY 6, June, 1979.

5. Bell, F., Estimating Design Floods From Extreme Rainfall, Hydrology Papers, Colorado State University Fort Collins, Colorado, No. 29, June 1968.

6. Beven, K., On the Generalized Kinematic Routing Method, Water Resources Research, Vol. 15, No. 5, October, 1979.

7. Bree, T., The General Linear Model With Prior Information, Journal of Hydrology, 39, Elsevier Scientific Publishing Company, Amsterdam, Printed in The Netherlands, pp. 113-127, 1978.

8. Cermak, R. and Feldman, A., Urban Hydrologic Modeling Using HEC-1/Kinematic Wave, Presented at the 19th Annual AWRA Conference, San Antonio, Texas, 1983.

9. Chien, J. and Sarikelle, S., Synthetic Design Hyetograph and Rational Runoff Coefficient, Journal of The Irrigation and Drainage Division, Vol. 102, No. IR3, September, 1976.

10. Chow, V.T. and Kulandaiwamy, V.C., The IUH of General Hydrologic System Model, Journal of The Hydraulics Division, ASCE, Vol. 108, No. HY7, pp 679-690, July, 1982.

11. Crippen, J., Envelope Curves For Extreme Flood Events, Journal of The Hydraulic Division, ASCE, Vol. 108, No. HY10, October, 1982.

12. Dawdy, D. and Bergmann, J., Effect of Rainfall Variability on Streamflow Simulation, Water Resources Research, Vol. 5, No. 5, October, 1969.

13. Dawdy, D. and O'Donnell, T., Mathematical Models of Catchment Behavior, Journal of The Hydraulics Division, ASCE, Vol. 91, No. HY4, July, 1965.

14. Debo, T., Urban Flood Damage Estimating Curves, Journal of The Hydraulics Division, ASCE, Vol. 108, No. HY10, October, 1982.

15. Dickinson, W., Holland, M.E. and Smith, G.L., An Experimental Rainfall-Runoff Facility, No. 25, Hydrology Papers, Colorado State University, Fort Collins, Colorado, September, 1967.

16. Fleming G. and Franz, D., Flood Frequency Estimating Techniques For Small Watersheds, Journal of The Hydraulics Division, ASCE, Vol. 97, No. HY9, September, 1971.

17. Fogel, M. and Duckstein, L., Point Rainfall Frequencies in Convective Storms, Water Resources Research, Vol. 5, No. 6, December, 1969.

18. Garen, D. and Burges, S., Approximate Error Bounds for Simulated Hydrographs, Journal of The Hydraulics Division, ASCE, Vol. 107, No. HY11, November, 1981.

19. Gundlach, A., Adjustment of Peak Discharge Rates for Urbanization, Journal of The Irrigation and Drainage Division, ASCE, Vol. 104, No. IR3, September, 1978.

20. Gupta, V. and Sorooshian, S., Uniqueness and Observability of Conceptual Rainfall-Runoff Model Parameters: The Percolation Process Examined, Water Resources Research, Vol. 19, pp 269-276, 1983.

21. Hjalmarson, H., Flash Flood in Tanque Verde Creek, Tucson, Arizona, Journal of Hydraulic Engineering, Vol. 110, No. 12, December 1984.

22. Hjelmfelt, A., Convolution and The Kinematic Wave Equations, Journal of Hydrology, 75, Elsevier Science Publishers, B.V., Amersterdam, Printed in The Netherlands, pp. 301-309, (1984/1985).

23. Hjemlfelt, A. and Burwell, R., Spatial Variability of Runoff, Journal of Irrigation and Drainage Engineering, ASCE, Vol. 110, No. IR1, March 1984.

24. Hollis, G., The Effect of Urbanization on Floods of Different Recurrence Interval, Water Resources Research, Vol. 11, No. 3, June, 1975.

25. Hornberger, G.H., Beven, K.J., Cosby, B.J. and Sappington, D.E., Shenandoah Water Shed Study: Calibration of A Topography-Based, Variable Contributing Area Hydrological Model to a Small Forested Catchment, Water Resources Research, Vol. 21, No. 12, pp 1841-1850, December, 1985.

26. Huang, Y., Channel Routing By Finite Difference Method, Journal of The Hydraulics Division, Vol. 104, No. HY10, October, 1977.

27. Johnston, P. and Pilgrim, D., Parameter Optimization for Watershed Models, Water Resources Research, Vol. 12, No. 3, pp 477-486, June, 1976.

28. Katopodes, N., Schamber, D., Applicability of Dam-Break Flood Wave Models, Journal of Hydraulic Engineering, Vol. 109, No. 5, May, 1983.

29. Keefer, T.N., Comparison of Linear Systems and Finite Differences Flow-Routing Techniques, Water Resources Research, Vol. 12, No. 5, pp 997-1006, October, 1976.

30. Kelway, P., The Rainfall Recorder Problem, Journal of Hydrology, 26, Elsevier Scientific Publishing Company, Amsterdam, Printed in The Netherlands, pp 55-77, 1975.

31. Kite, G., Confidence Limits for Design Events, Water Resources Research, Vol. 11, No. 1, February, 1975.

32. Klemes, V. and Bulu, A., Limited Confidence in Confidence Limits Derived by Operational Stochastic Hydrologic Models, Journal of Hydrology, 42, Elsevier Scientific Publishing Company, Amsterdam, Printed in The Netherlands, pp 9-22, 1979.

33. Lee, L. and Essex, T., Urban Headwater Flooding Damage Potential, Journal of Hydraulic Engineering, ASCE, Vol. 109, No. HY4, April, 1983.

34. Loague, K. and Freeze, R., A Comparison of Rainfall-Runoff Modeling Techniques on Small Upland Catchments, Water Resources Research, Vol. 21, No. 2, pp 229-248, February, 1985.

35. Mawdsley, J. and Tagg, A., Identification of Unit Hydrographs From Multi-Event Analysis, Journal of Hydrology, 49, Elsevier Scientific Publishing Company, Amsterdam, Printed in The Netherlands, pp. 315-327, 1981.

36. Mays, L.W. and Coles, L., Optimization of Unit Hydrograph Determination, Journal of The Hydrualics Division, ASCE, Vol. 106, No. HY1, pp 85-91, January, 1980.

37. Mays, L. and Taur, C., Unit Hydrograph via Nonlinear Programming, Water Resources Research, Vol. 18, No. 4, pp. 744-752, August 1982.

38. McCuen, R.H. and Bondelid, T.R., Estimating Unit Hydrograph Peak Rate Factors, Journal of Irrigation and Drainage Division, ASCE, Vol. 109, No. IR2, June, 1983.

39. McCuen, R., et al, Estimating Urban Time of Concentration, Journal of Hydraulic Engineering, ASCE, Vol. 110, No. HY7, July, 1984.

40. McCuen, R., et al, SCS Urban Peak Flow Methods, Journal of Hydraulic Engineering, ASCE, Vol. 110, No. HY3, March, 1984.

41. McCuen, R.H., Yen, C.C., and Hromadka II, T.V., "Adjusting Stream Gage Data for Urbanization Effects", Mocrosoftware for Engineers, 1986.

42. McPherson, M. and Schneider W., Problems in Modeling Urban Watersheds, Water Resources Research, Vol. 10, No. .3, June, 1974.

43. Mein, R.G. and Brown, B.M., Sensitivity of Optimized Parameters in Watershed Models, Water Resources Research, Vol. 14, No. 2, April, 1978.

44. Nash, J. and Sutcliffe, J., River Flow Forecasting Through Conceptual Models Part 1 - A Discussion of Principles, Journal of Hydrology, Vol. 10, pp 282-290, 1970.

45. Neff, E., How Much Rain Does a Rain Gage Gage?, Journal of Hydrology, 35, Elsevier Scientific Publishing Company, Amsterdam, Printed in The Netherlands, pp 213-220, 1977.

46. Osborn, H. and Hickok, R., Variability of Rainfall Affecting Runoff From A Seminarid Rangeland Watershed, Southwest Watershed Research Center Tucson, Arizona, Water Resources Research, Vol. 4, No. 1, February, 1968.

47. Osborn, H. and Lane, L., Precipitation - Runoff for Very Small Semiarid Rangeland Watersheds, Water Resources Research, Vol. 5, No. 2, April, 1969.

48. Pedersen, J., et al, Hydrographs by Single Linear Reservoir Model, Journal of The Hydraulics Division, ASCE, Vol. 106, No. HY5, May, 1980.

49. Pilgrim, D., Travel Times and Nonlinearity of Flood Runoff From Tracer Measurements on a Small Watershed, Water Resources Research, Vol. 12, No. 3, June, 1976.

50. Pitman, W., Flow Generation By Catchment Models of Differing Complexity - A Comparison of Performance, Journal of Hydrology, 38, Elsevier Scientific Publishing Company, Amsterdam, Printed in The Netherlands, pp. 59-70, 1978.

51. Porter, J.W., A Comparison of Hydrologic and Hydraulic Catchment Routing Procedures, Journal of Hydrology, 24, pp 333-349, 1975.

52. Reed, D., et al, A Non-Linear Rainfall-Runoff Model, Providing For Variable Lag Time, Journal of Hydrology, 25, North-Holland Publishing Company, Amsterdam, Printed in The Netherlands, pp. 295-305, 1975.

53. Rose, F. and Hwang, G., A Study of Differences Between Streamflow Frequency and Rainfall Frequency for Small Rural Watersheds, 1985 International Symposium on Urban Hydrology, Hydraulic Infrastructures and Water Quality Control, University of Kentucky, July, 1985.

54. Ruh-Ming, Li, et al, Nonlinear Kinematic Wave Approximation for Water Routing, Water Resources Research, Vol. 11, No. 2, April, 1975.

55. Schilling, W. and Fuchs, L., Errors in Stormwater Modeling - A Quantitative Assessment, Journal of The Hydraulics Division, ASCE, Vol. 112, No. HY2, pp 111-123, February, 1986.

56. Scully, D.R. and Bender, D.L., Separation of Rainfall Excess from Total Rainfall, Water Resources Research, Vol. 5, No. 4, pp 877-883, August, 1969.

57. Sorooshian, S. and Gupta, V., Automatic Calibration of Conceptual Rainfall-Runoff Models: The Question of Parameter Observability and Uniqueness, Water Resources Research, Vol. 19, No. 1, pp 260-268, February, 1983.

58. Stedinger, J., Confidence Intervals for Design Events, Journal of Hydraulic Engineering, ASCE, Vol. 109, No. HY1, January, 1983.

59. Stedinger, J., Design Events with Specified Flood Risk, Water Resources Research, Vol. 19, No. 2, pp. 511-522, April, 1983.

60. Tingsanchali T. and Manandhar, S., Analytical Diffusion Model for Flood Routing, Journal of Hydraulic Engineering, ASCE, Vol. 111, No. HY3, March, 1985.

61. Troutman, B., An Analysis of Input in Perception-Runoff Models Using Regression With Errors in the Independent Variables, Water Resources Research, Vol. 18, No. 4, pp 947-964, August, 1982.

62. U.S. Army Corps of Engineers, The Hydrologic Engineering Center, Hydrologic Engineering Methods for Water Resources Development: Volume 5 - Hypothetical Floods, Vol. 5, March, 1975.

63. U.S. Army Corps of Engineers, The Hydrologic Engineering Center, Continuous Hydrologic Simulation of The West Branch DuPage River Above West Chicago: An Application of Hydrocomp's HSP, Research Note No. 6, 1979.

64. U.S. Army Corps of Engineers, The Hydrologic Engineering Center, Adoption of Flood Flow Frequency Estimates at Ungaged Locations, Training Document No. 11, February 1980.

65. U.S. Army Corps of Engineers, The Hydrologic Engineering Center, Comparative Analysis of Flood Routing Methods, Research Document No. 24, September, 1980.

66. U.S. Army Corps of Engineers, The Hydrologic Engineering Center, Hydrologic Analysis of Ungaged Watersheds Using HEC-1, Training Document No. 15, 1982.

67. U.S. Army Corps of Engineers, The Hydrologic Engineering Center, Testing of Several Runoff Models on an Urban Watershed, Technical Paper No. 59, 1978.

68. U.S. Army Corps of Engineers, The Hydrologic Engineering Center, Introduction and Application of Kinematic Wave Routing Techniques Using HEC-1, Training Document No. 10, May, 1979.

69. U.S. Department of Agriculture, Soil Conservation Service, National Engineering Handbook Section 4 (NEH-4) 210-V1 Amendment 5, Transmission Losses, Washington, DC, March, 1983.

70. United States Department of the Interior Geological Survey, A Digital Model for Streamflow Routing by Convolution Methods, U.S. Geological Survey Water-Resources Investigations Report 83-4160.

71. U.S. Department of Transportation, Federal Highway Administration, Hydrology, Hydraulic Engineering Circular No. 19, October, 1984.

72. Wallis, J. and Wood, E., Relative Accuracy of Log Pearson III Procedures, Journal of Hydraulic Engineering, ASCE, Vol. 111, No. HY7, July, 1985.

73. Watt, W. and Kidd, C., Quurm-A Realistic Urban Runoff Model, Journal of Hydrology, 27, Elsevier Scientific Publishing Company, Amsterdam, Printed in The Netherlands, pp. 225-235, 1975.

74. Weinmann, E. and Laurenson, E., Approximate Flood Routing Methods: A Review, Journal of The Hydraulics Division, ASCE, Vol. 105, No. HY12, December, 1979.

75. Whitley, R.J. and Hromadka II, T.V., Computing Confidence Intervals for Floods I and II, Microsoftware for Engineers 2, pp 138-150 and 151-158, 1986.

76. Williams, D.W., Cameron, R.J. and Evans, G.P., TRRL and Unit Hydrograph Simulations Compared with Measurements in an Urban Catchment, Journal of Hydrology, 48, Elseview Scientific Publishing Company, Amsterdam, Printed in The Netherlands, pp 63-70, 1980.

77. Zaghloul, N., SWMM Model and Level of Discretization, Journal of The Hydraulics Division, ASCE, Vol. 107, No. HY11, November, 1981.

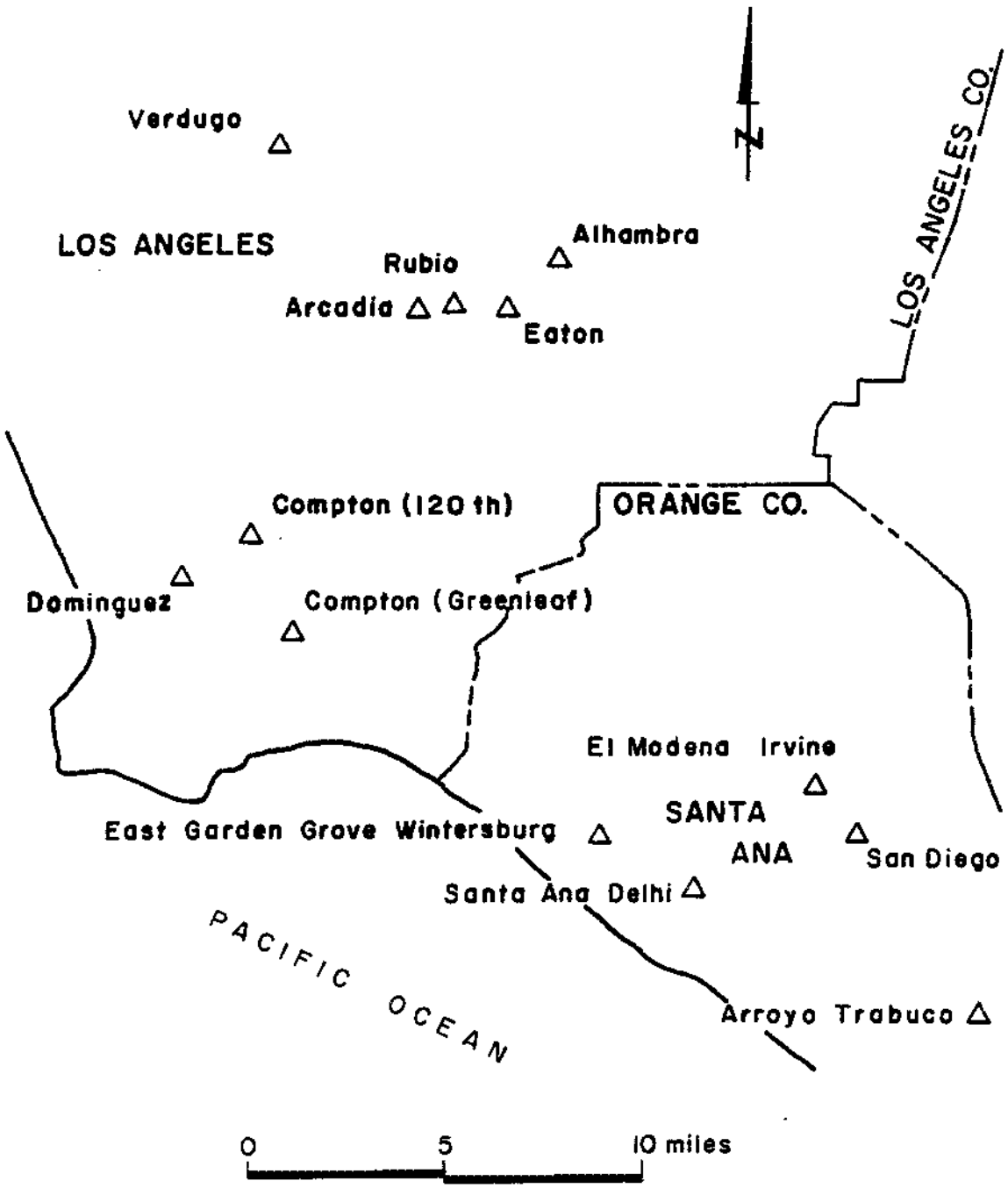

Fig. 1. Location of Drainage Basins.

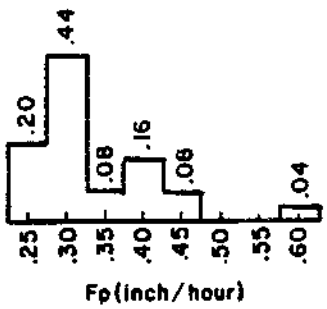

Fig. 2. HISTOGRAM OF SOIL LOSS FUNCTION

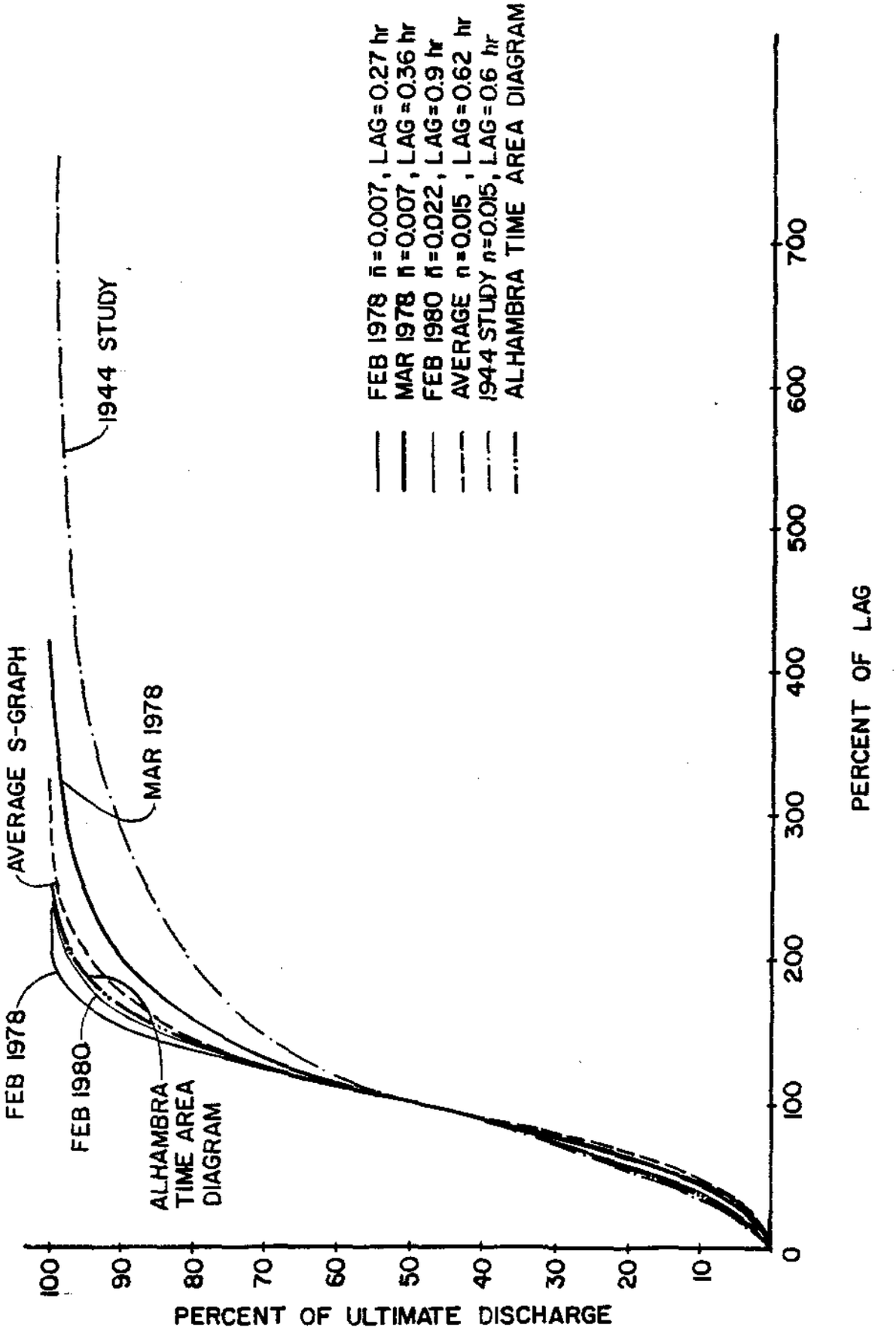

Fig. 3. Alhambra Wash S-Graphs.

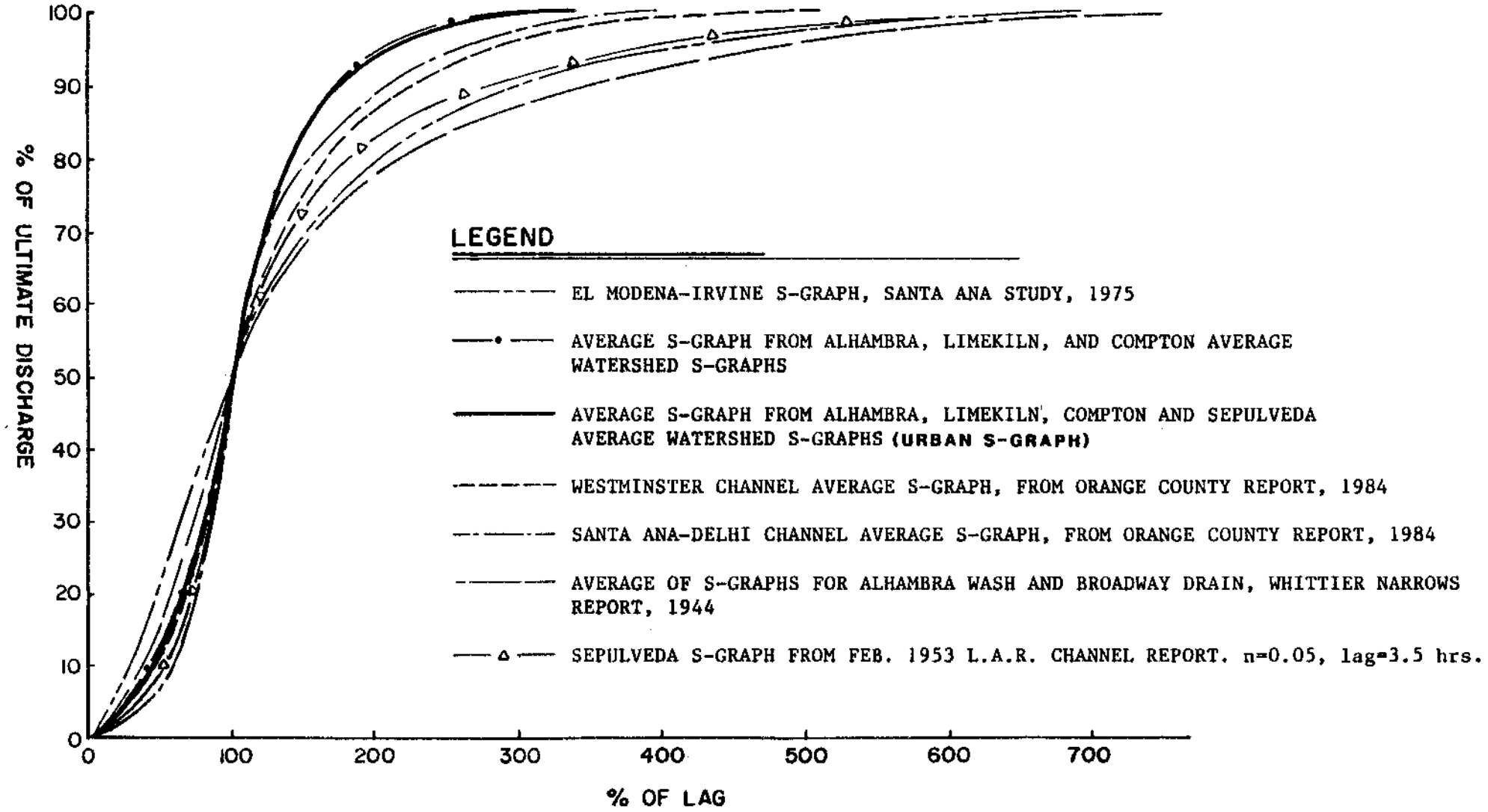

Fig. 4. Avarage S-Graphs.

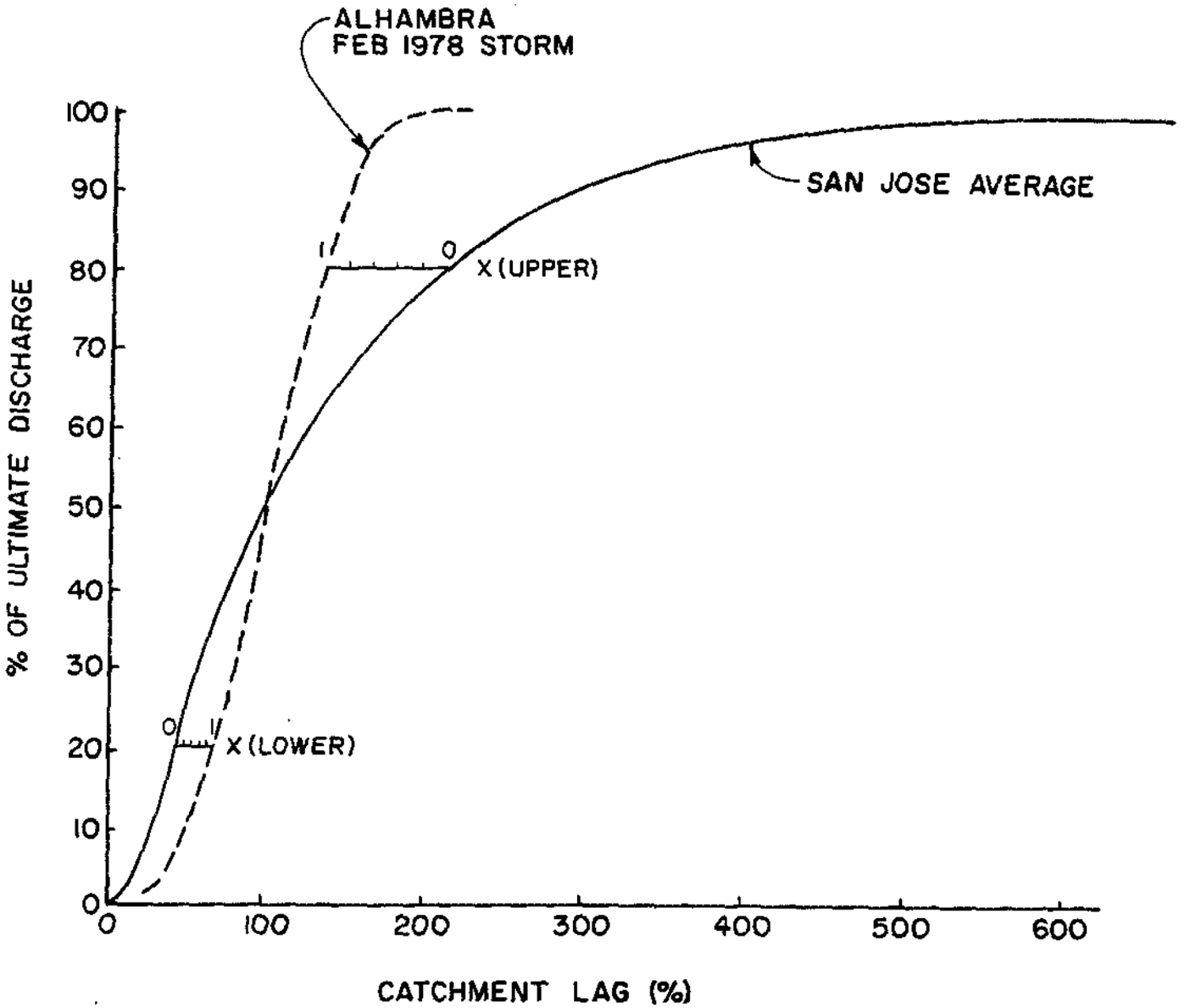

Fig. 5. S-Graph Scaling for S(X).

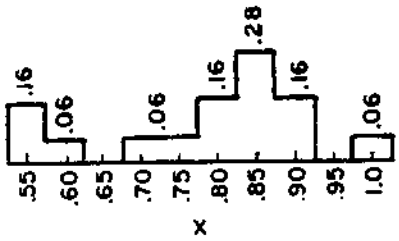

Fig. 6. HISTOGRAM OF VARIATION IN S-GRAPH

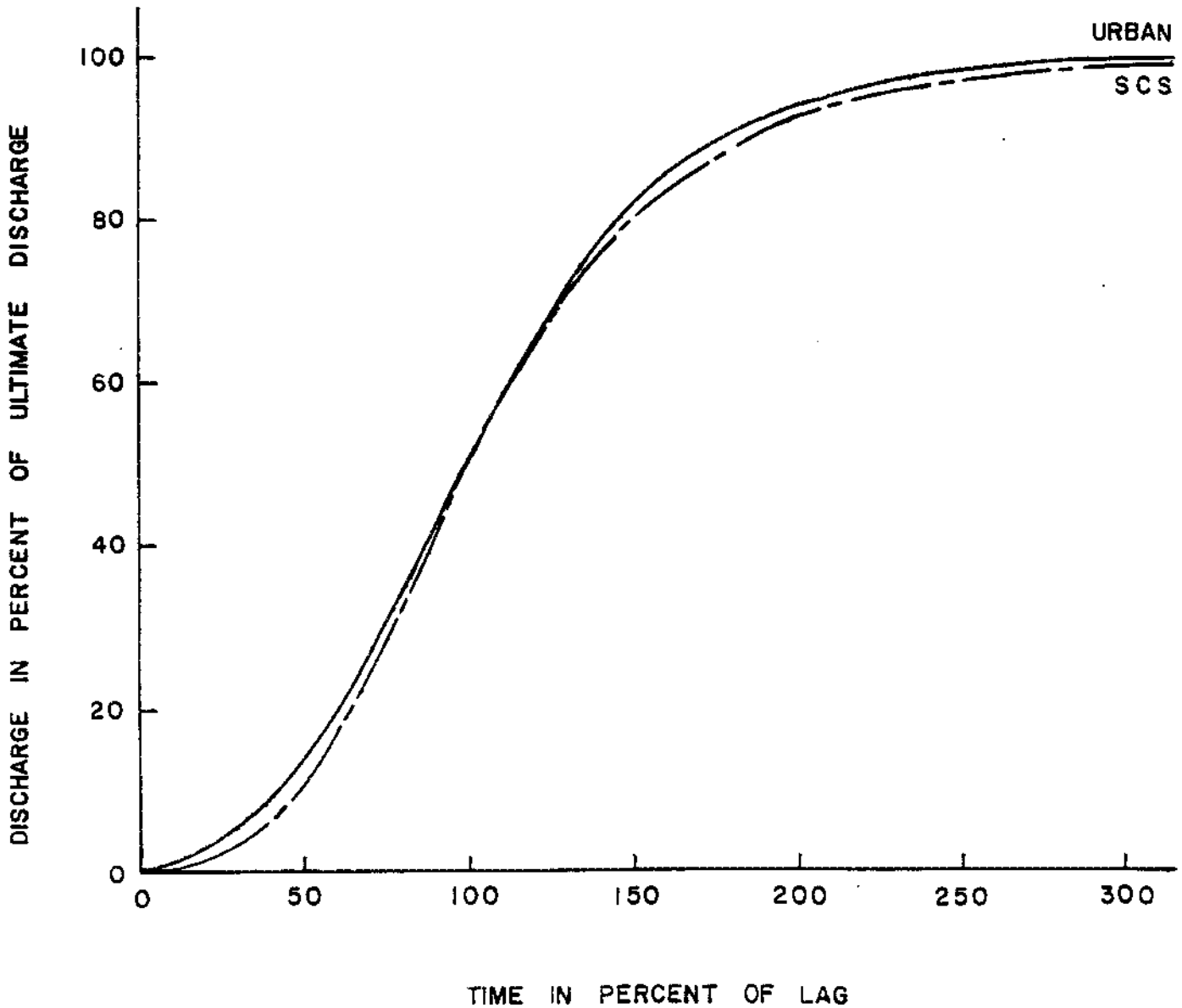

Fig. 7. Comparison of SCS and Urban S-Graphs.

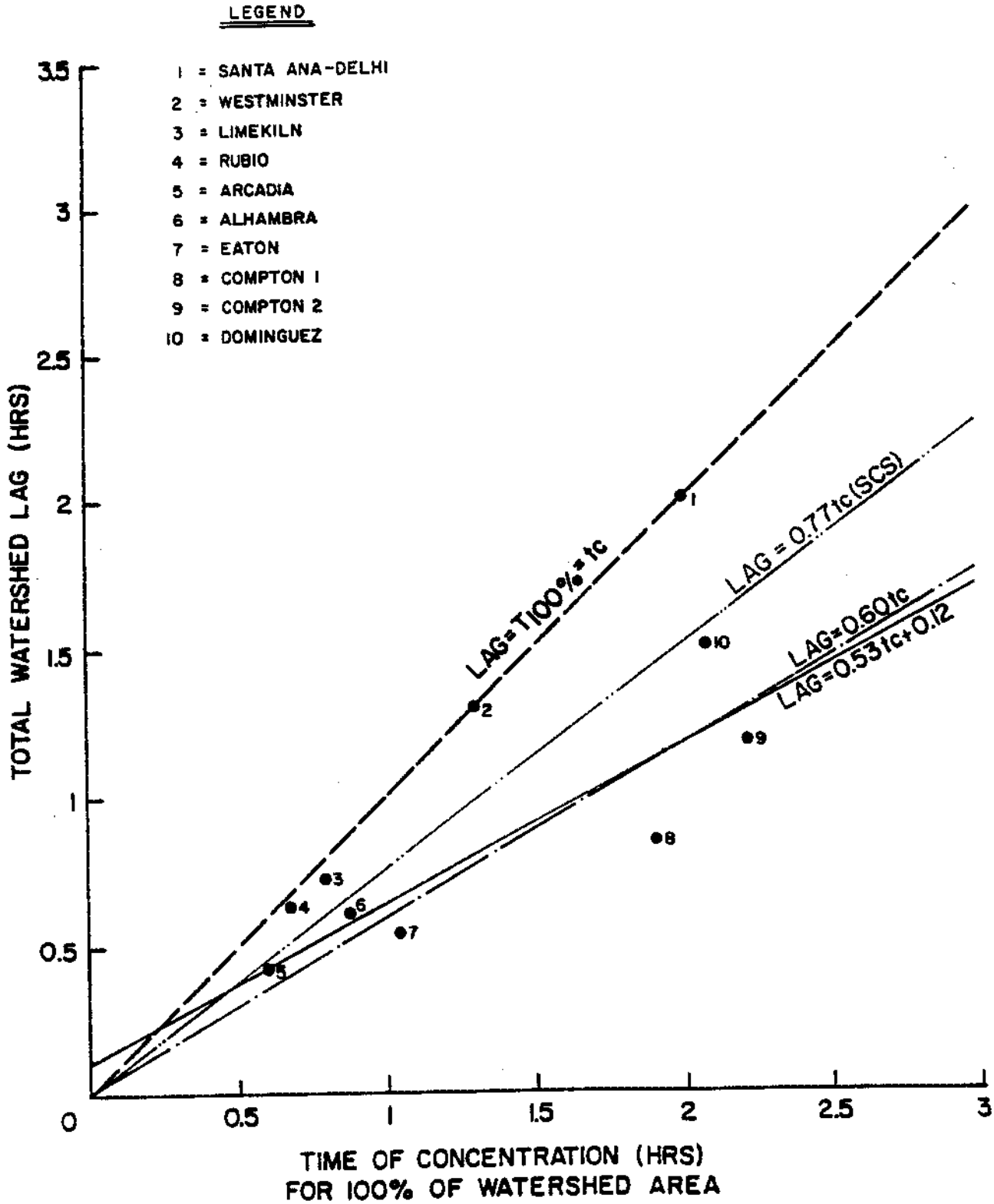

Fig. 8. Relationship Between Catchment Lag and Tc Values for Local Region.

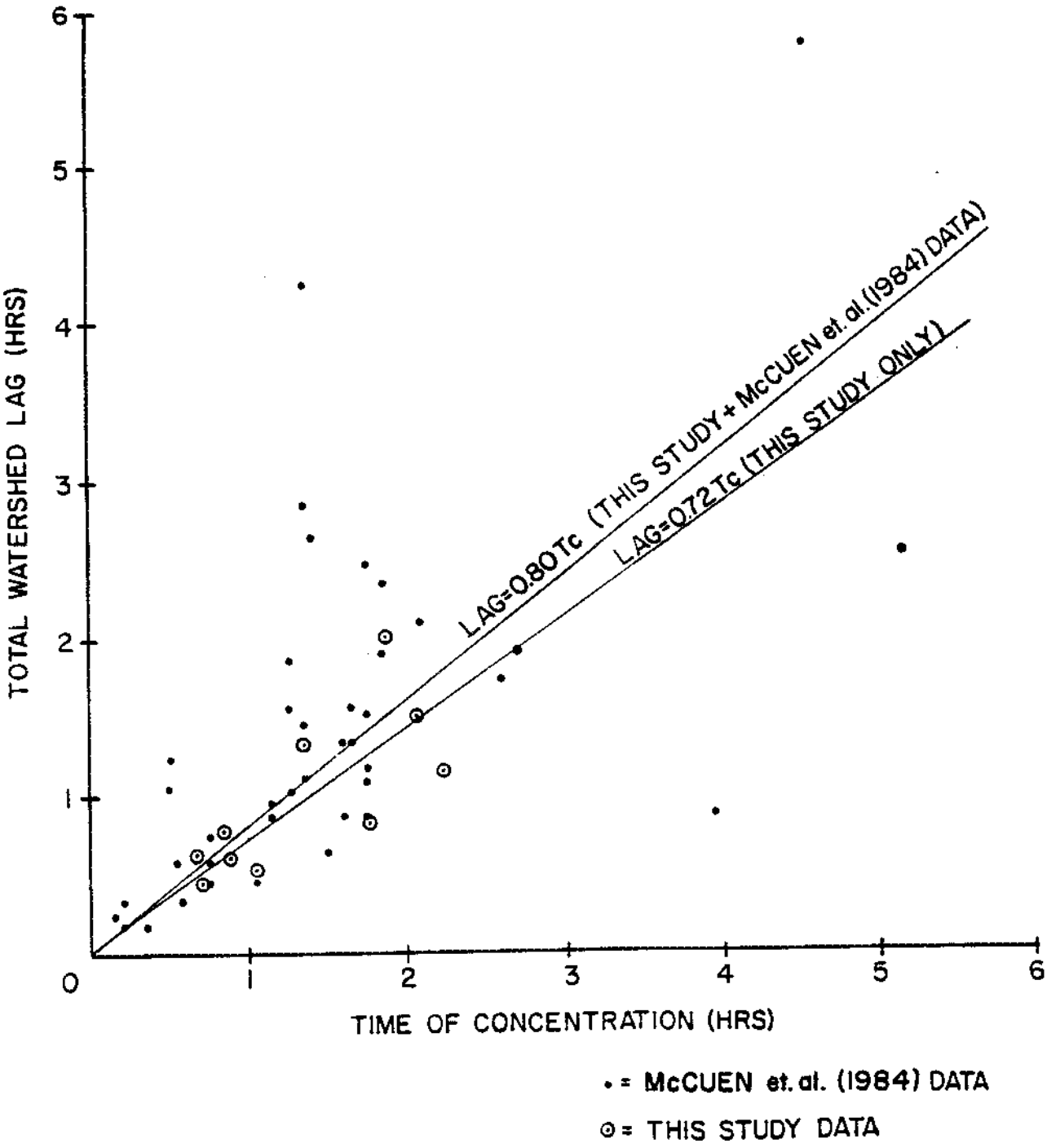

Fig. 9. Relationship Between Measured Catchment Lag and Computed Tc.

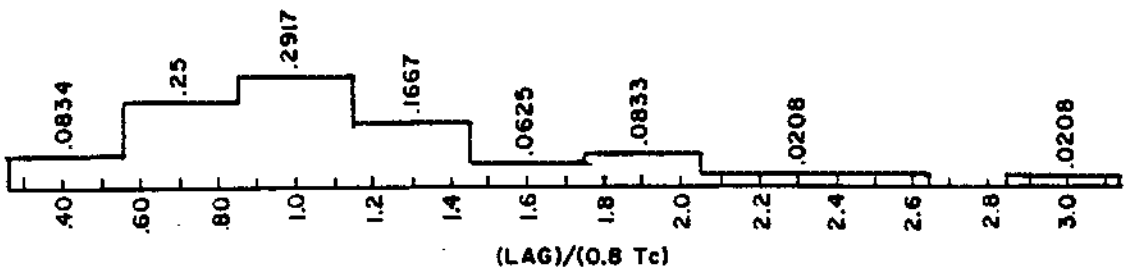

Fig. IQ HISTOGRAM OF LAG TIME

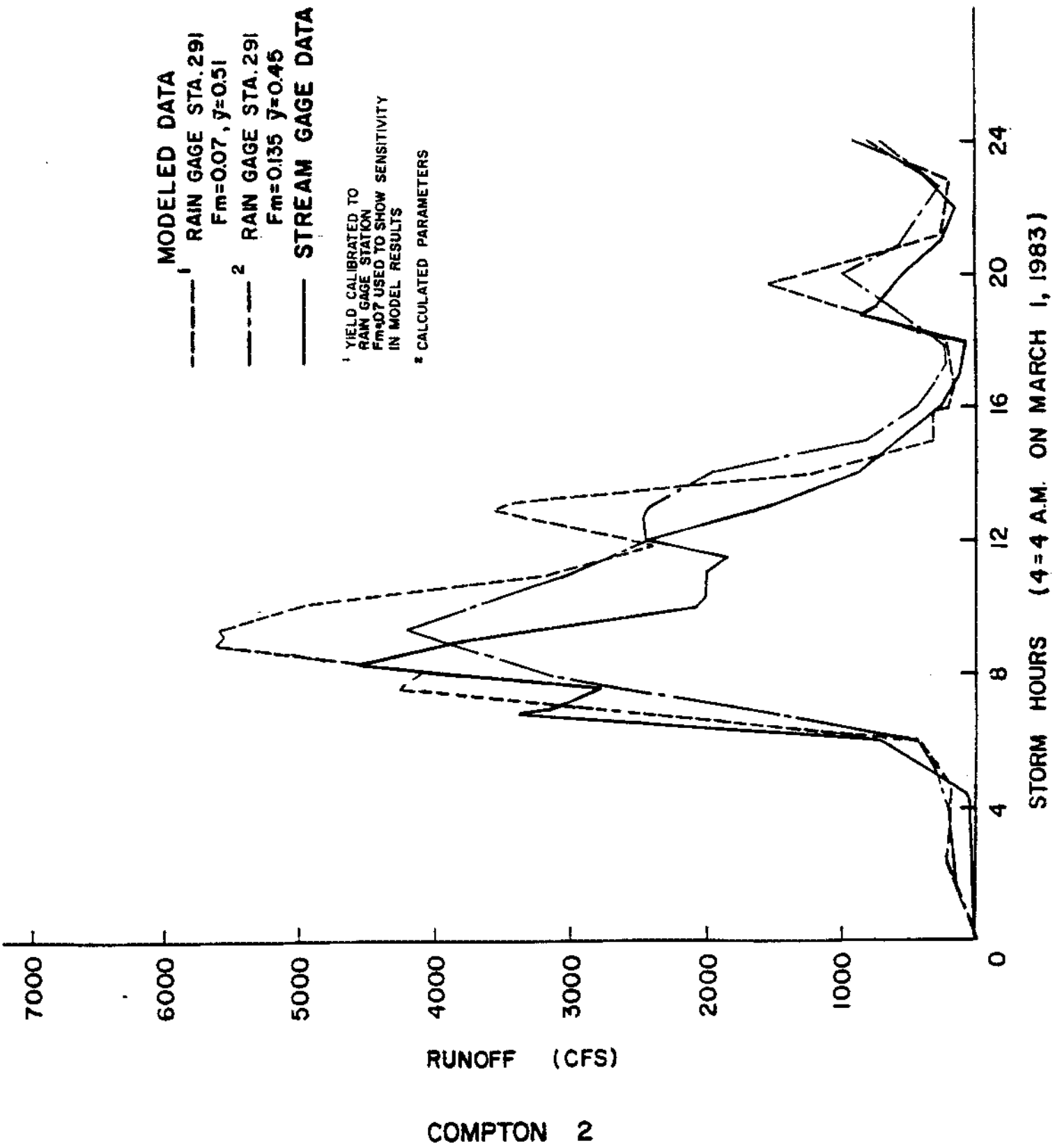

Fig. 11a. March 1, 1983 Runoff Hydrographs (1 of 6).

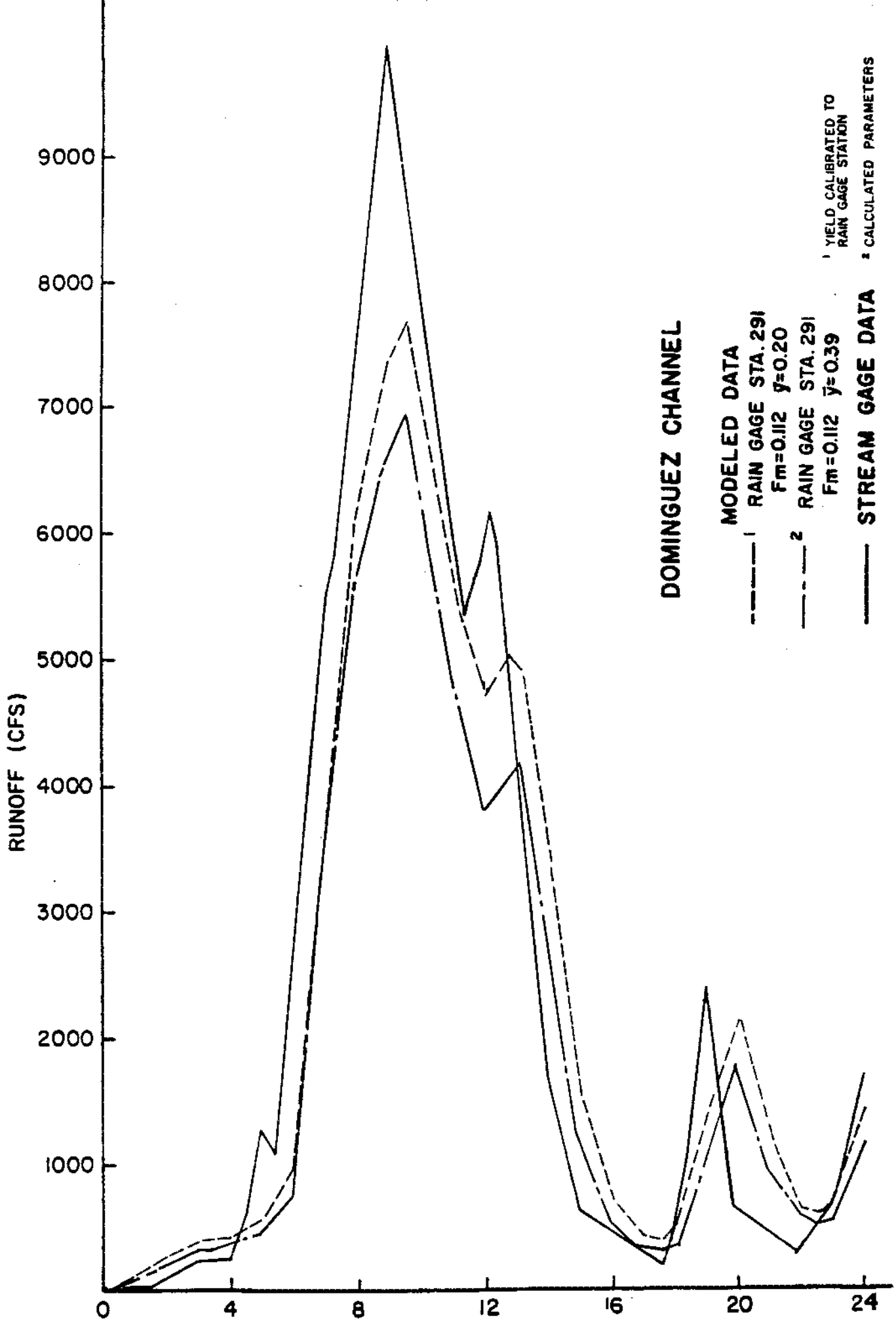

Fig. 11a. March 1, 1983 Runoff Hydrographs (2 of 6).

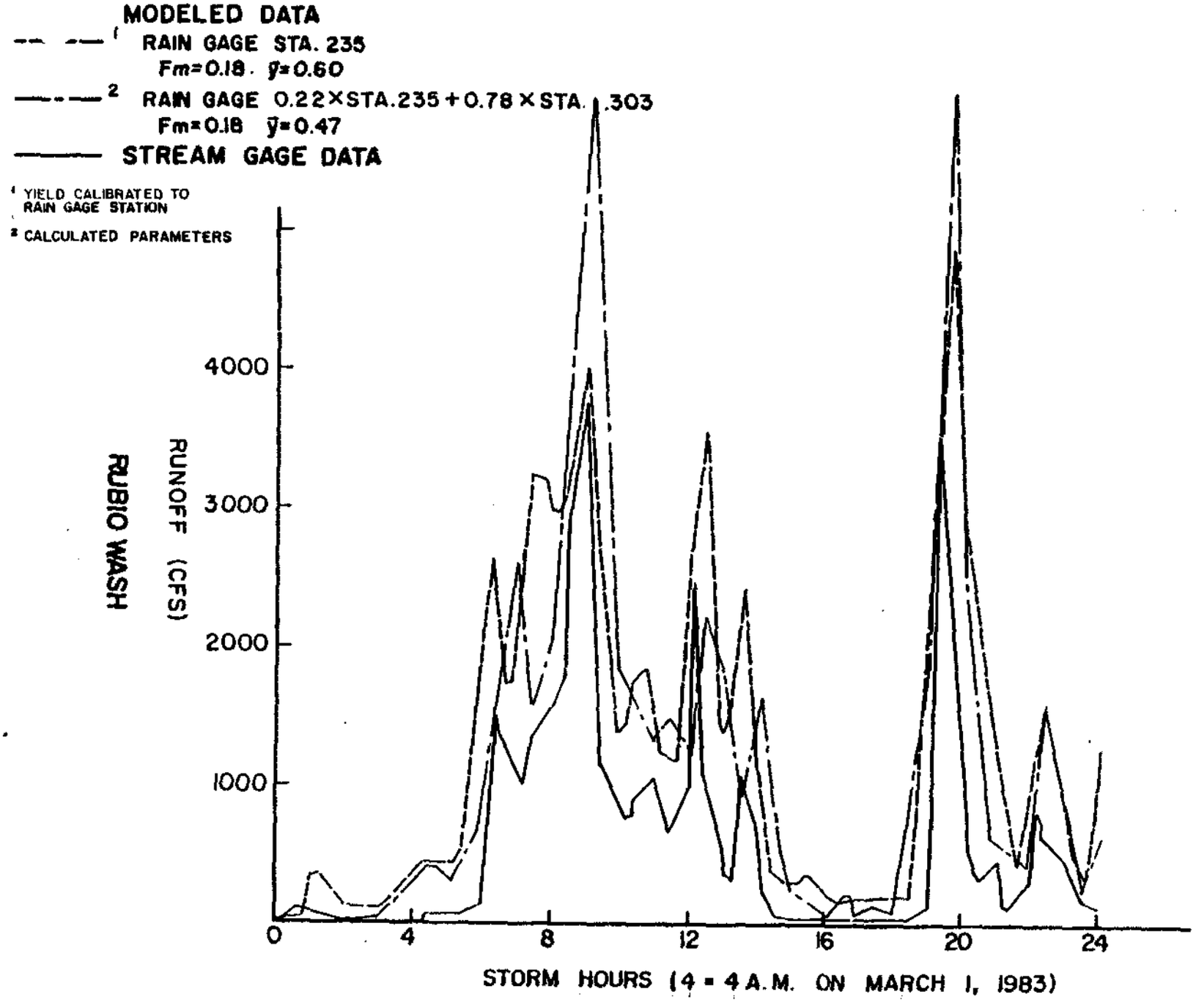

Fig. 11a. March 1, 1983 Runoff Hydrographs (3 of 6).

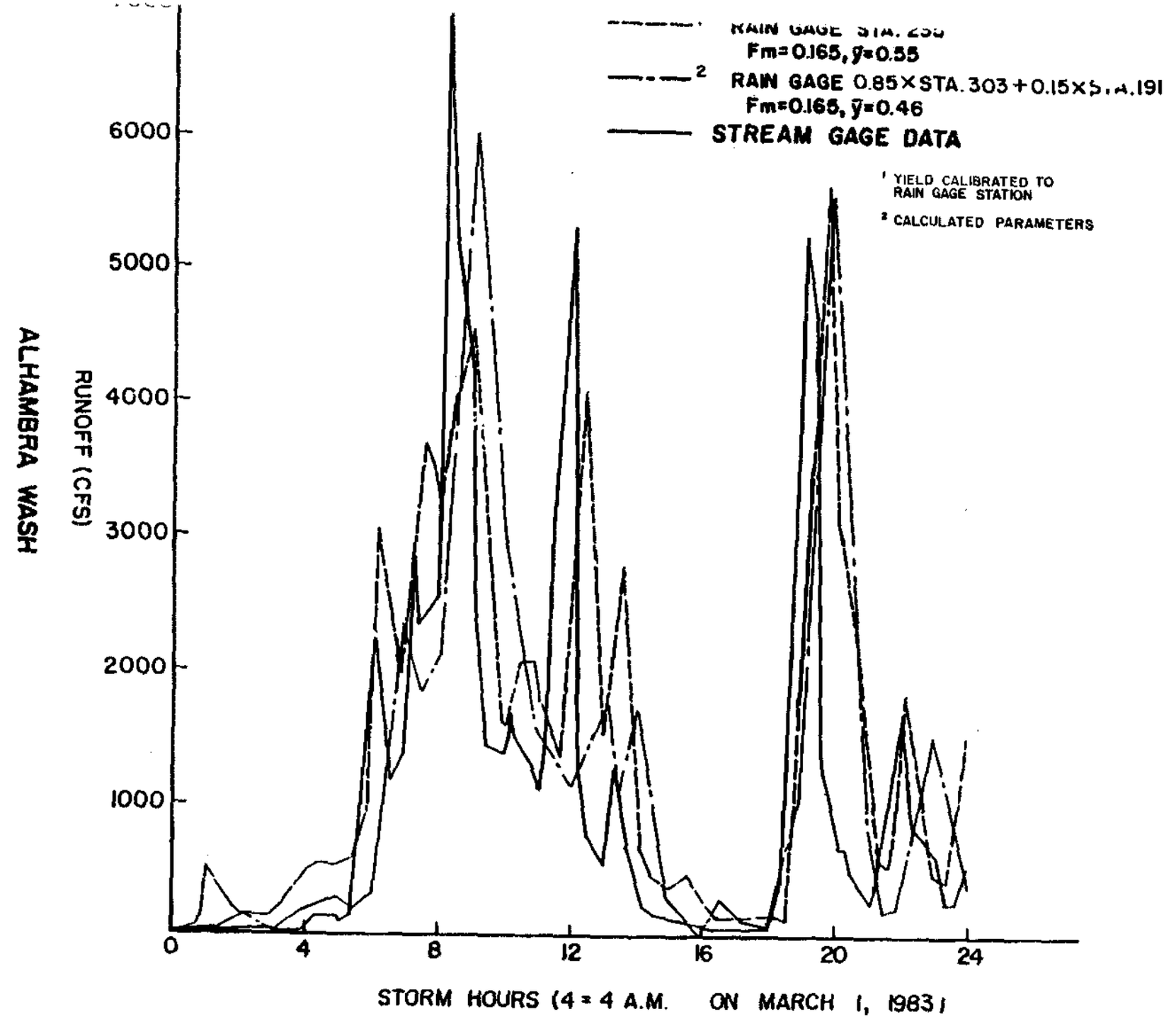

Fig. 11a. March 1, 1983 Runoff Hydrographs (4 of 6).

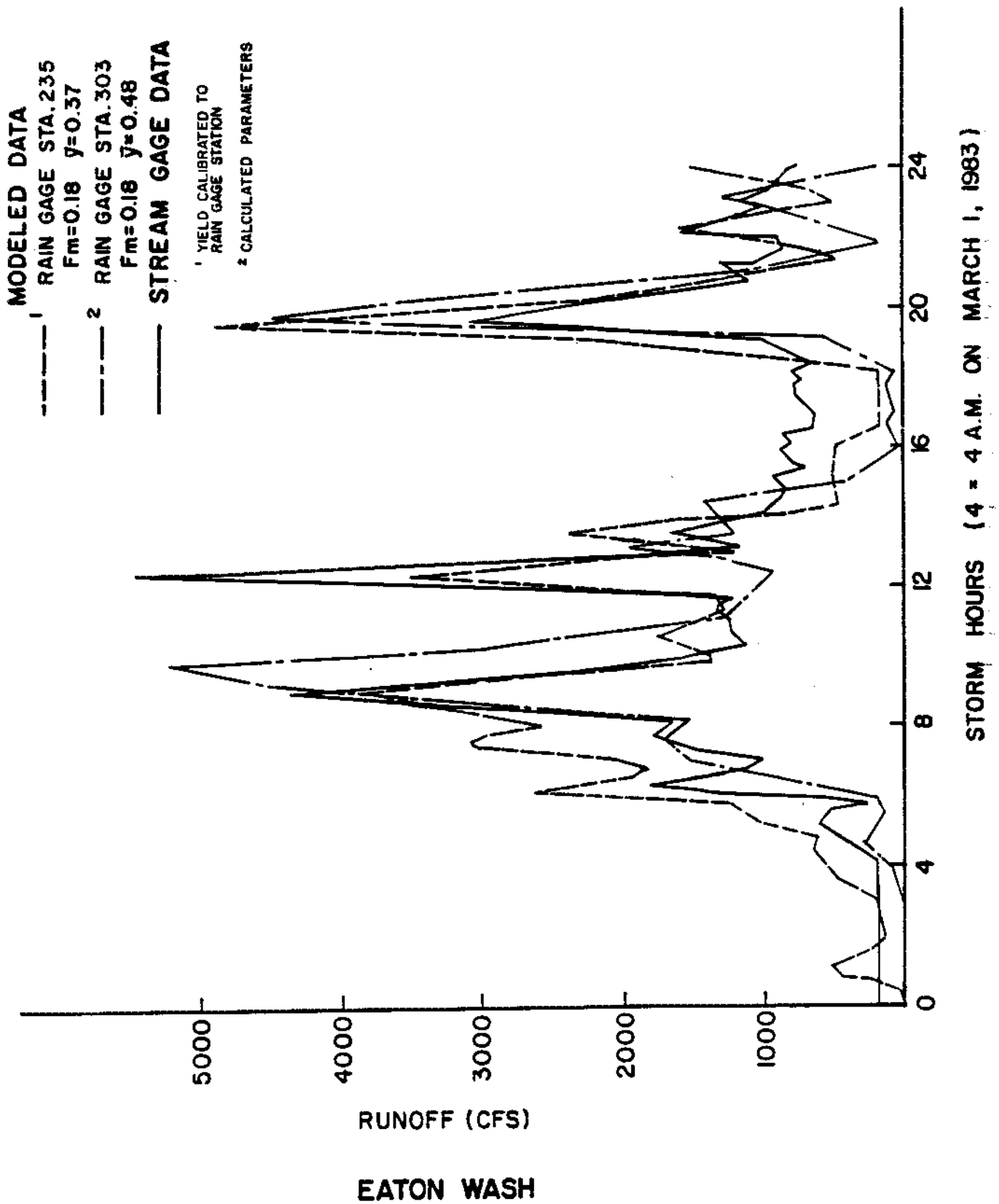

Fig. 11a. March 1, 1983 Runoff Hydrographs (5 of 6).

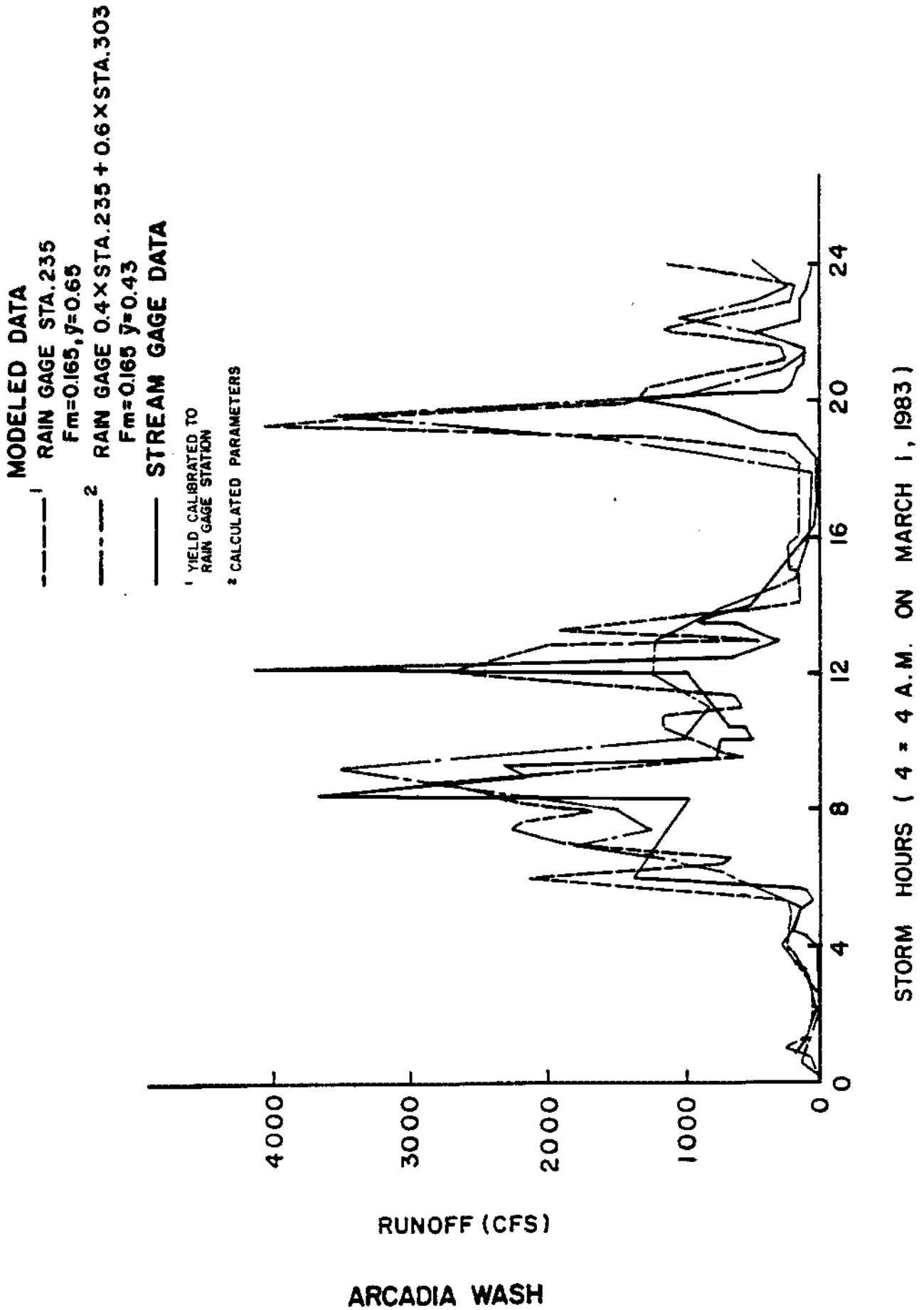

Fig. 11a. March 1, 1983 Runoff Hydrographs (6 of 6).

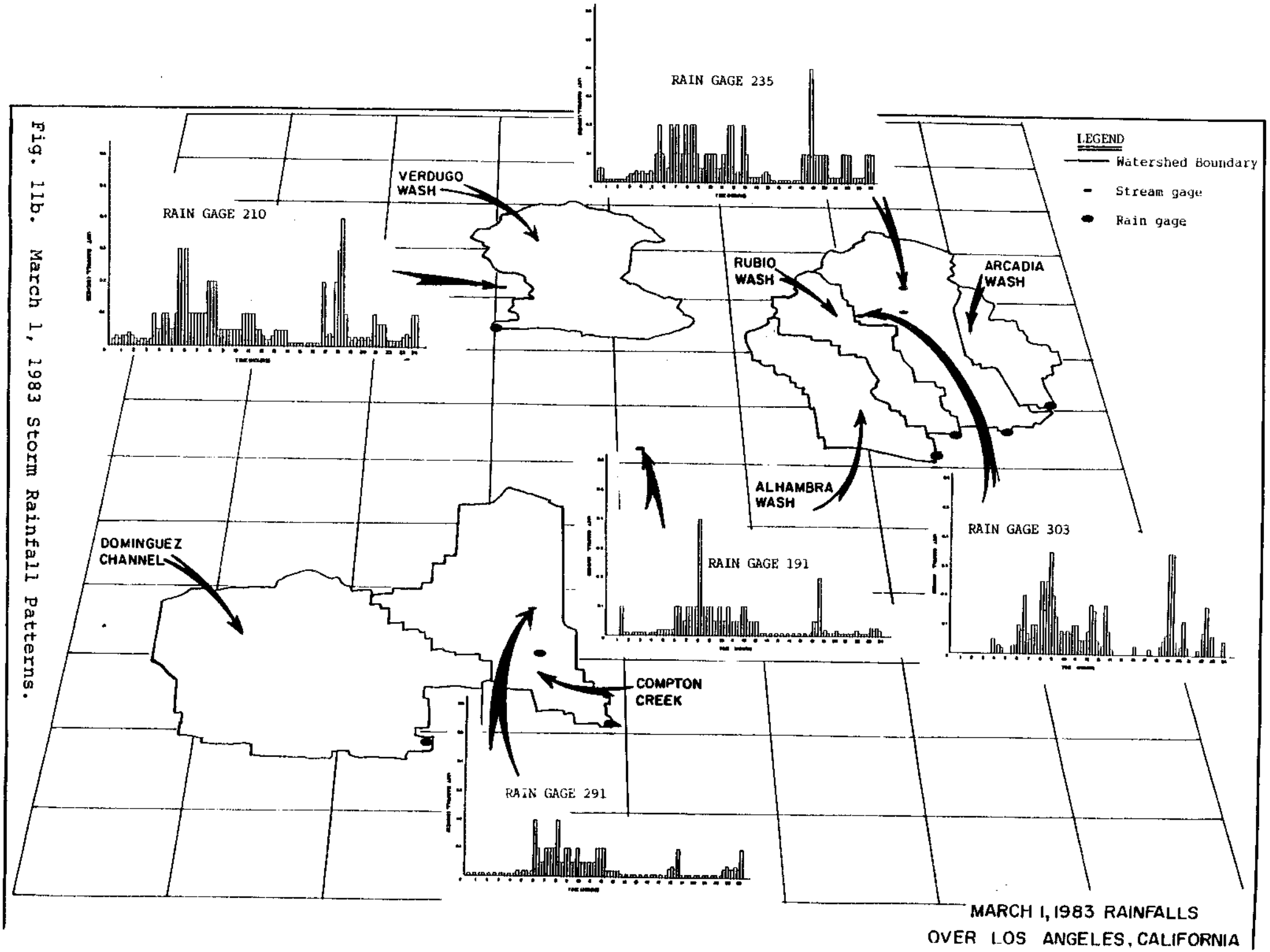

Fig. 11b. March 1, 1983 Storm Rainfall Patterns.

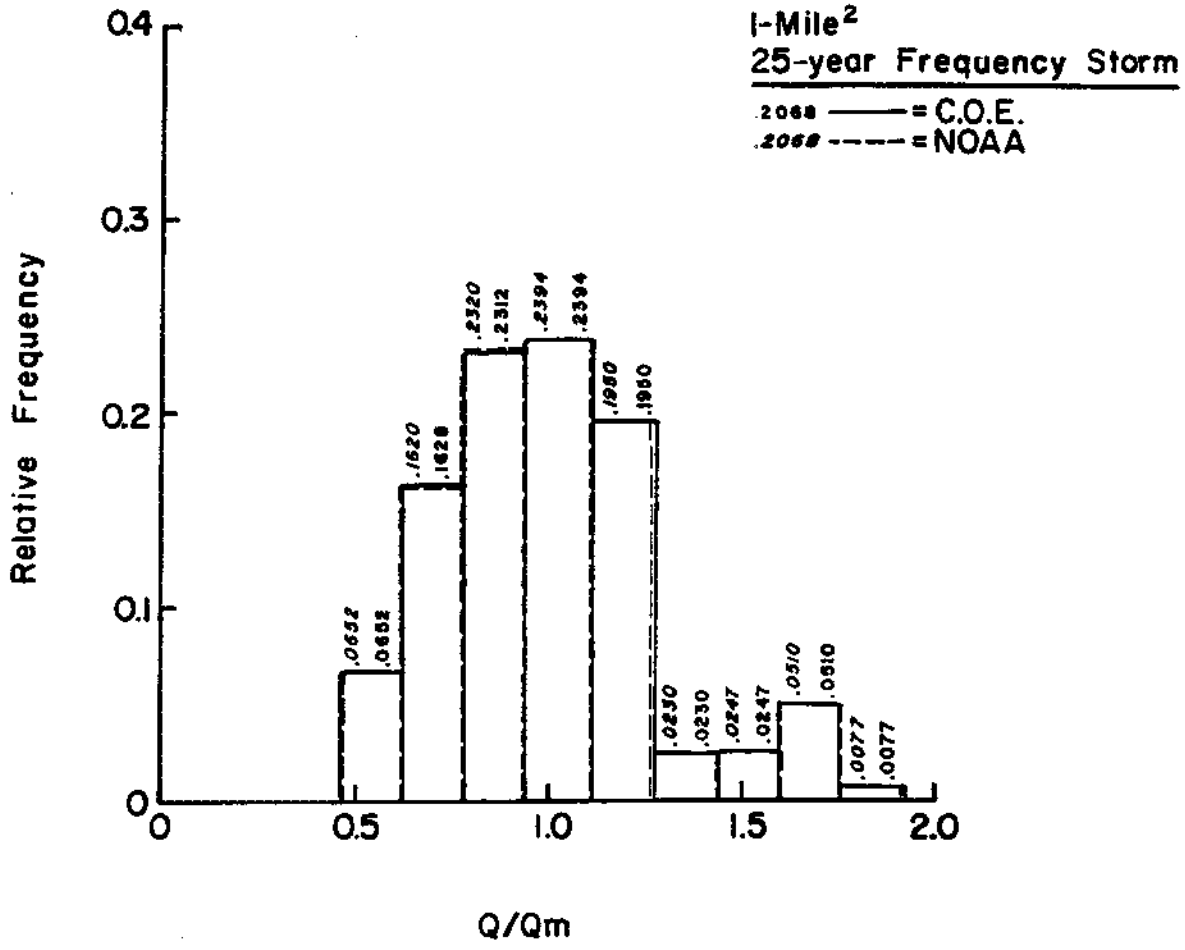

Fig. 12. Q/Qm Distribution for Tc= 1-hour, Area= 1-mi.^{2}, and COE or NOAA Depth-Area Adjustments.

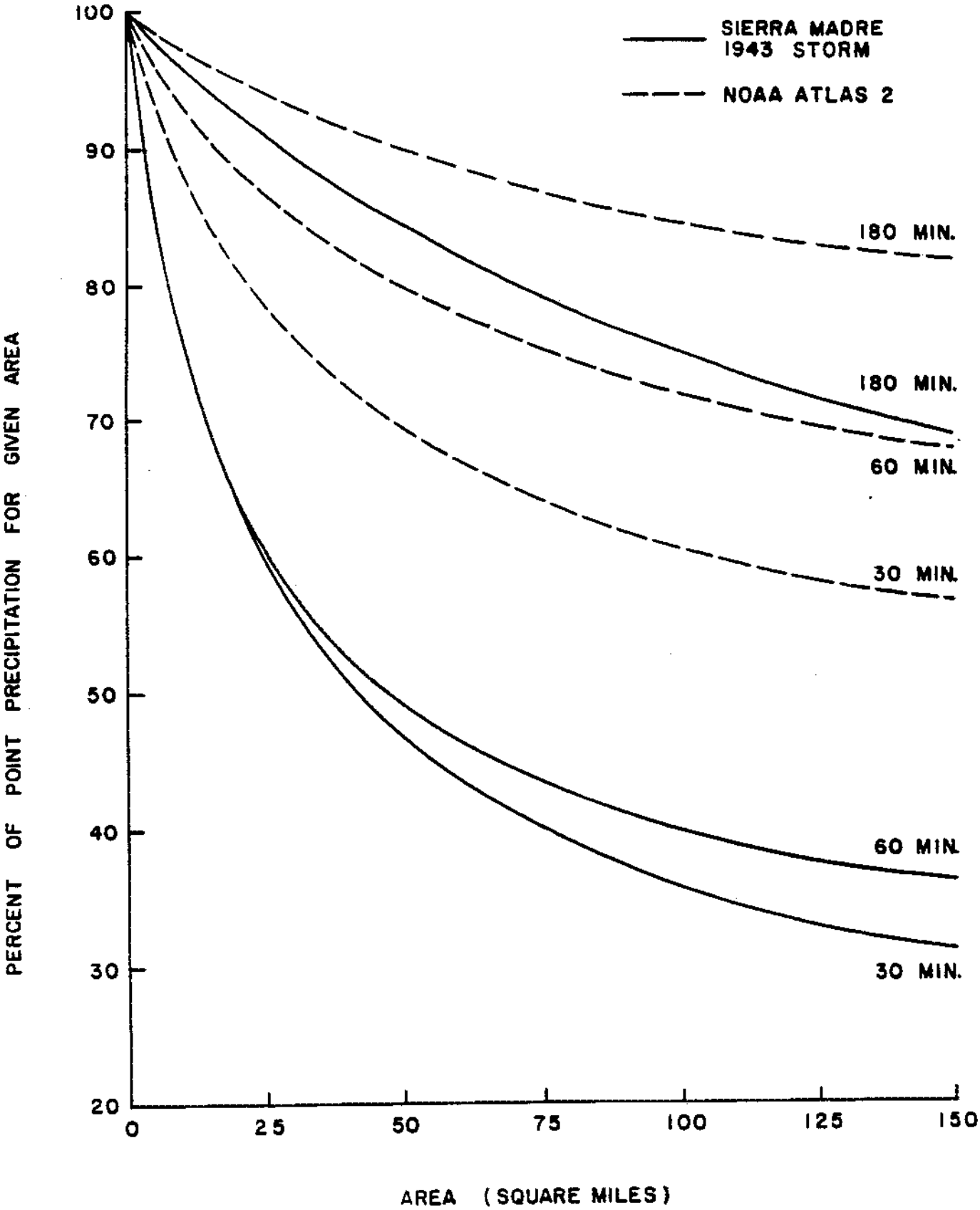

Fig. 13. Depth-Area Adjustment Curves.

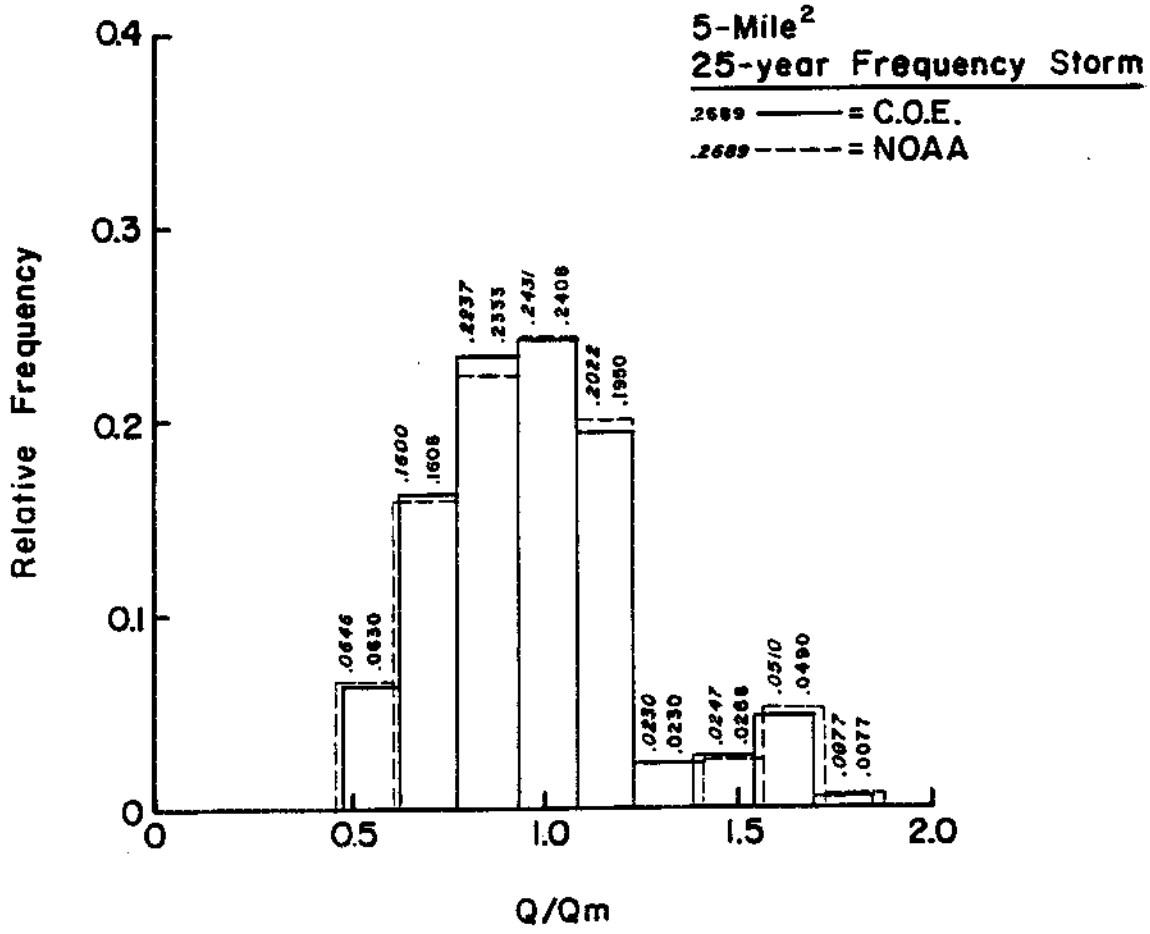

Fig. 14. Q/Qm Distribution for 5-mi.^{2} Area.

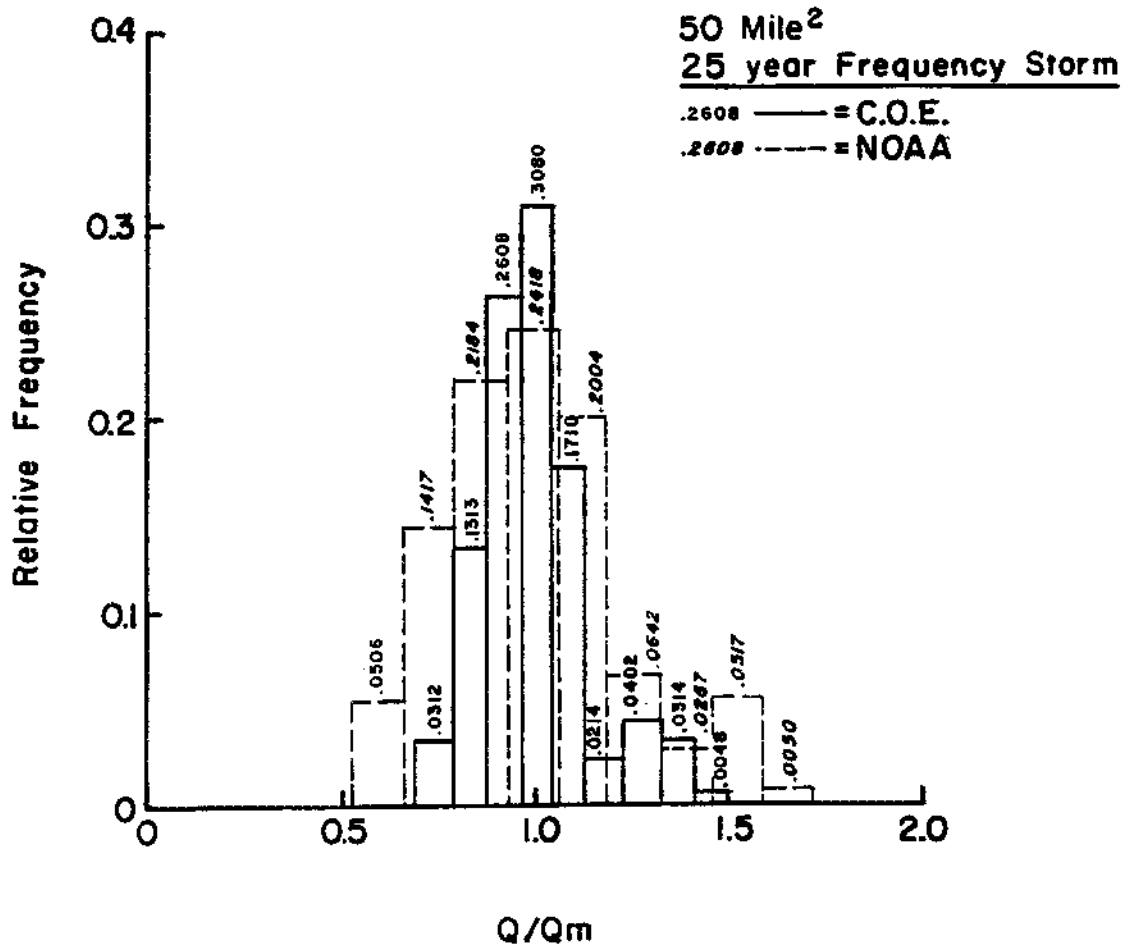

Fig. 15. Q/Qm Distribution for 50-mi.^{2} Area.

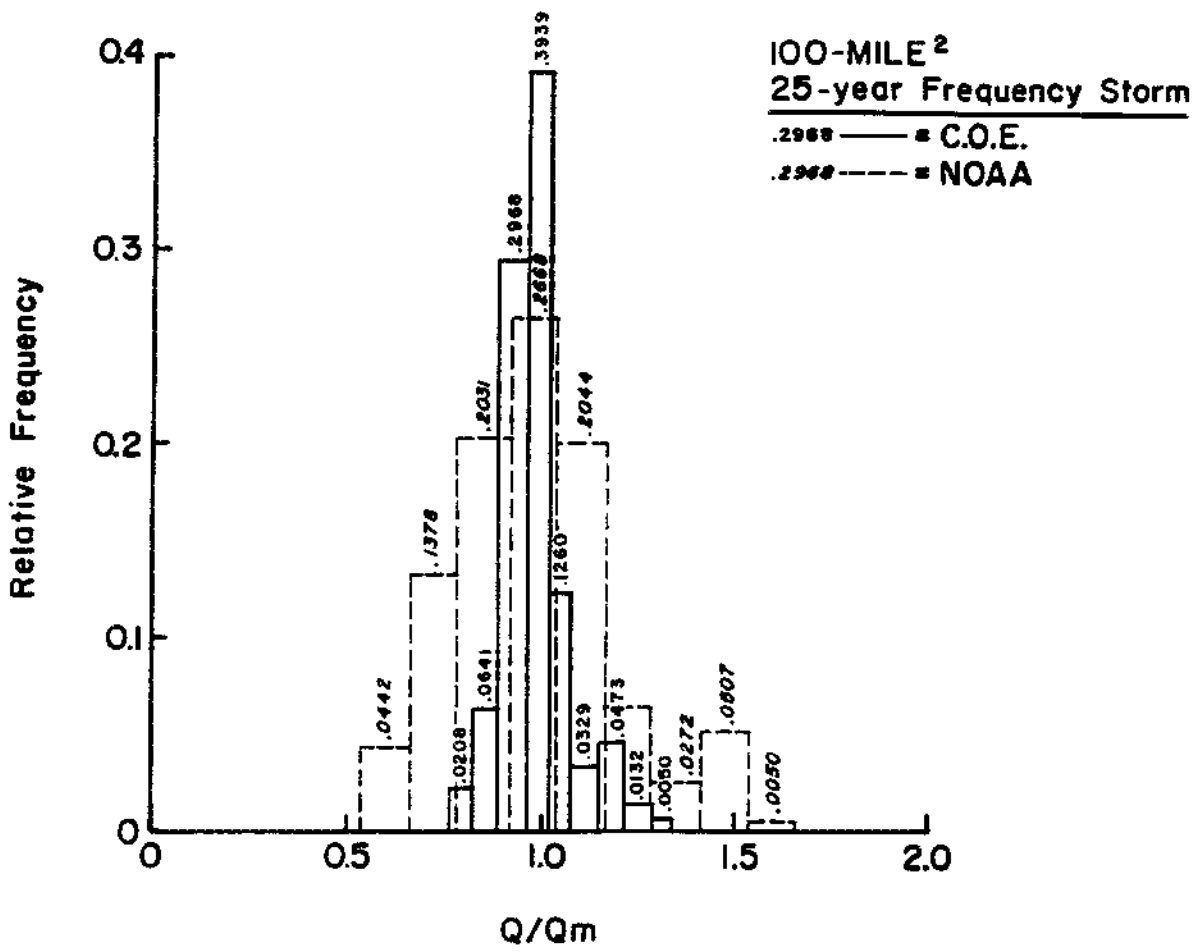

Fig. 16. Q/Qm Distribution for 100-mi.^{2} Area.

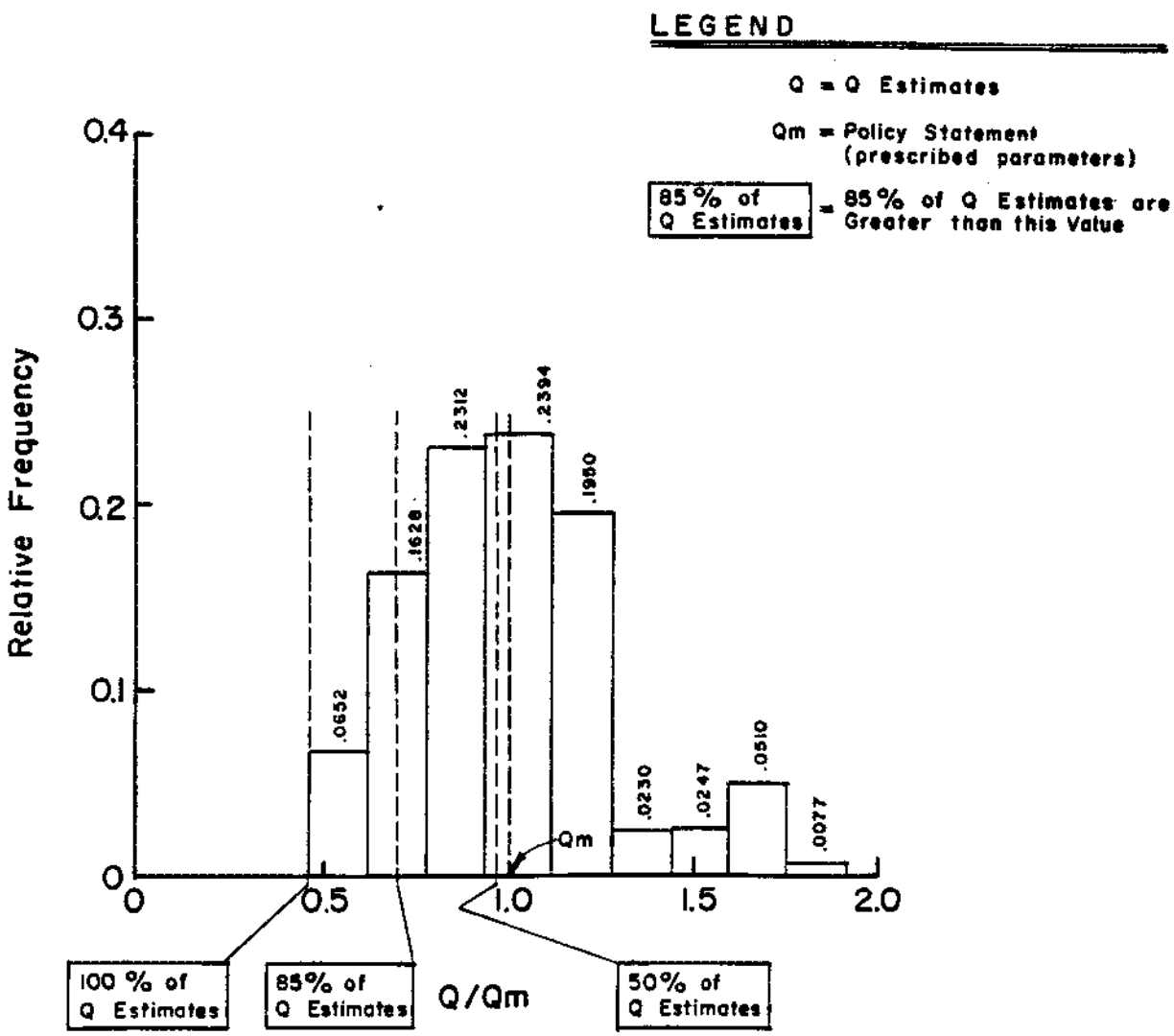

Fig. 17 Interpretation of Q/Qm Distribution and Model Uncertainty.

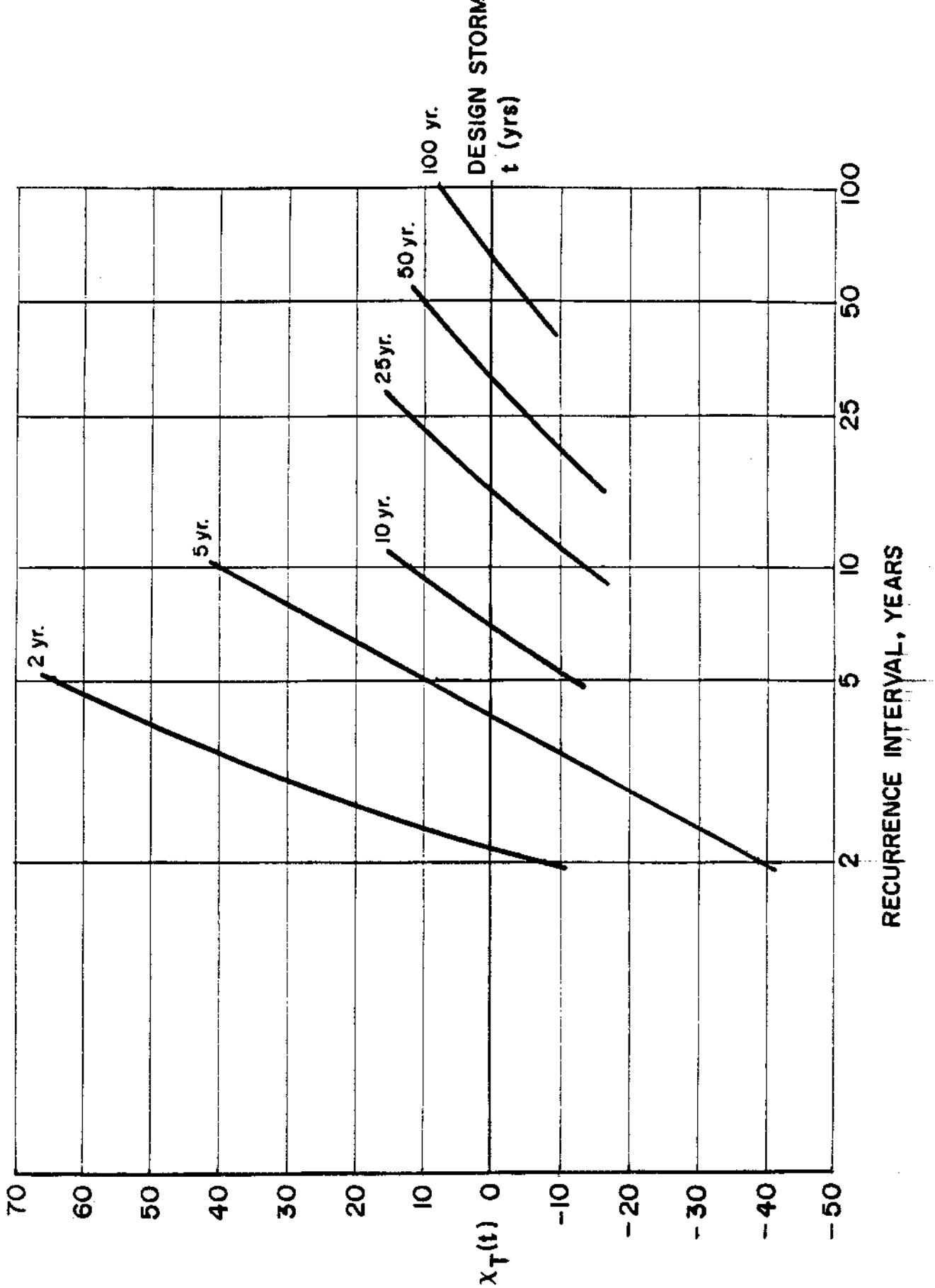

Fig. 18 Design Storm Calibration Results.

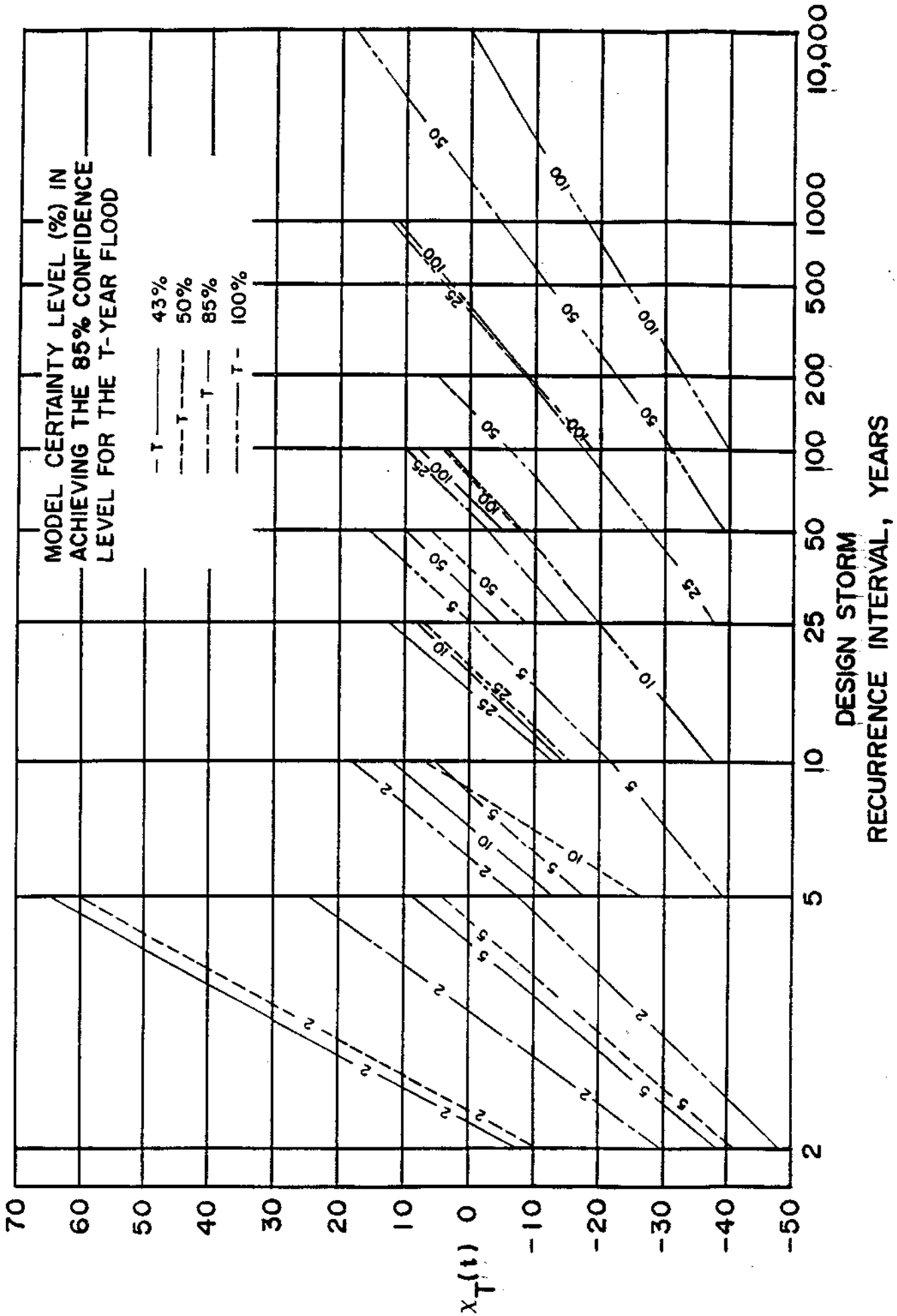

Fig. 19. Evaluation of Model Certainty in Predicting T-Year Floods.